Accepted Manuscript

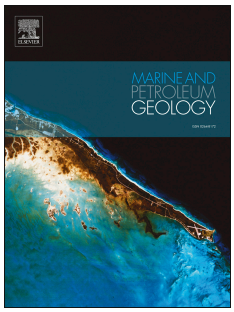

A dual-porosity model for evaluating petroleum resource potential in unconventional tight-shale plays with application to Utica Shale, Quebec (Canada)

Zhuoheng Chen, Denis Lavoie, Michel Malo, Chunqing Jiang, Hamed Sanei, Omid H. Ardakani

PII: S0264-8172(16)30440-8

DOI: 10.1016/j.marpetgeo.2016.12.011

Reference: JMPG 2759

To appear in: *Marine and Petroleum Geology*

Received Date: 18 July 2016

Revised Date: 12 December 2016

Accepted Date: 14 December 2016

Please cite this article as: Chen, Z., Lavoie, D., Malo, M., Jiang, C., Sanei, H., Ardakani, O.H., A dual-porosity model for evaluating petroleum resource potential in unconventional tight-shale plays with application to Utica Shale, Quebec (Canada), *Marine and Petroleum Geology* (2017), doi: 10.1016/j.marpetgeo.2016.12.011.

A dual-porosity model for evaluating petroleum resource potential in unconventional tight-shale plays with application to Utica Shale, Quebec (Canada)

Zhuoheng Chen[1], Denis Lavoie[2], Michel Malo[3], Chunqing Jiang[1], Hamed Sanei[1] and Omid H. Ardakani[1]
[1]Geological Survey of Canada, 3303-33rd Street, NW, Calgary, AB, T2L 2A7 Canada
[2]Geological Survey of Canada, 490 de la Couronne, Québec, Qc, G1K 9A9, Canada
[3]Institut National de la Recherche Scientifique, Eau Terre Environnement, 490 de la Couronne, Québec, Qc G1K 9A9Canada
zhuohengchen@canada.c.ca

Abstract

Unconventional tight to shale reservoirs vary from tight sandstone/siltstone to organic-rich mudstone/shale, commonly with mixed lithologies. In such reservoir systems, matrix pores and organic pores with different origins and distinct physical and chemical properties co-exist for hydrocarbon storage. Traditional resource assessment methods, designed for conventional reservoirs, cannot handle the two pore systems properly. This study proposes a dual-porosity model to respond to the need for a new method in assessing hydrocarbon resource potential in such reservoir systems. The dual-porosity model treats the two types of pores separately and derives the resource estimates from different sources of data, thus better characterizing unconventional reservoirs with complicated pore systems. The new method also has the flexibility of assessing resource potential for the entire spectrum of mixed lithologies ranging from a complete tight to a pure source rock (organic–rich shale/mudstone) reservoir. The proposed method is illustrated through the assessment of the in-place petroleum resource potential in the Upper Ordovician Utica Shale of southern Quebec, Canada. The results of the application suggest that the proposed approach effectively handles the two pore systems in tight-shale reservoirs effectively and provides a useful tool for estimating resource potential in unconventional plays.

Key Words: matrix pore, organic pore, volumetric, kerogen kinetics

Highlights

Tight-shale reservoir contains mixed pore systems with different origins and distinct physical/chemical properties

Conventional method of resource assessment cannot adequately address the complexity of mixed storages in tight-shale reservoir

An innovative method is proposed for handling mixed storage for improving resource evaluation in unconventional reservoir

Pore type and quantities of resource in each pore system provide information useful for resource development planning

Introduction

Recent advances in horizontal drilling coupled with multistage hydraulic fracturing enable commercial oil and gas production from unconventional reservoirs. Unconventional tight to shale reservoirs are low porosity-permeability, fine-grained rocks with lithological characteristics ranging from typical tight sandstone/siltstone to organic rich laminae in mudstone/shale (CSUG, 2010; Passey, et al. 2010; Jarvie, 2012a; Bohacs et al. 2013). The spatial heterogeneity of reservoir can be seen from altering lithologies, mineral composition and content, rock mechanics and texture of the reservoir rocks at various scales (e.g., Hill et al. 2007; Passey et. al. 2010; Aplin and Macquaker, 2011; Bohacs et al., 2013; Lei et al., 2015). The importance of these heterogeneities are indicated by drastic changes in production rates across tight and shale reservoirs (Maugeri, 2015; Chen and Hannigan, 2016). Organic rich shales have been traditionally regarded as the source rock in a conventional petroleum system (Tissot and Welte, 1984), and some of them are now considered as a self-sourced and self-contained, economically viable reservoir through long range horizontal drilling coupled with multi-stage hydraulic fracturing. The unconventional tight-shale resource play is usually a closed petroleum system with the crude oil and natural gas originating from the organic-rich shale directly in contact with the tight reservoir and being stored in both organic and inorganic matrix pores (including natural fractures) (Loucks, et al. 2009; Jarvie, 2012b; Modica and Lapierre, 2012).

Depending on the predominant lithology, mineralogy and thermal maturity, the matrix porosity may provide the principal storage for expelled petroleum, whereas additional petroleum remains within organic pores in the source rocks. A mixed storage system has important implications for resource evaluation. The two pore systems have different origins and show distinct physical and chemical properties, which imposes challenges to the characterization of reservoir properties using traditional methods. The matrix porosity is a function of mechanical and chemical compaction, where burial and basinal fluid histories are major controlling factors. In contrast, organic porosity is closely associated with hydrocarbon generation in the organic matter. Their abundance and characteristics are controlled by quantity, type and thermal maturity of the organic matter, and can be further complicated by preservation conditions. The current publicly available methods of assessing unconventional petroleum resources are either designed for matrix porosity of conventional reservoir without discriminating matrix porosity from

organic porosity (e.g., Ambrose et al., 2012) or consider organic porosity only (e.g., Modica and Lapierre, 2012). Recent studies of unconventional tight-shale reservoirs have generated new thoughts on their pore size distribution, pore structure and fluid thermo-dynamics (e.g., Loucks et al, 2009; Passey et al. 2010; Chalmers et al. 2012; Akkutlu and Fathi, 2012; Bohacs et al., 2013; Williams, 2013). These ideas form the basis for the development of a new resource evaluation scheme to handle challenges that are intrinsic to unconventional reservoirs and could significantly affect the resource potential estimate.

The objective of this paper is to discuss a dual-porosity model to address the need for a new method of assessing petroleum resources in unconventional reservoirs. In this article, we describe the dual porosity model and its application to tight-shale resource plays with reservoirs that contain mixed porous media as hydrocarbon storage with contrasting physical and chemical properties. Conceptual models for characterising storage in tight-shale reservoirs will be discussed first and the methodology description follows. The application is exemplified through the first evaluation of in-place hydrocarbon resource potential of the Upper Ordovician Utica Shale of the St. Lawrence Platform in southern Quebec, Canada.

Conceptual model for evaluating unconventional resources

General overview

Loucks et al. (2012) presented a pore classification based on pore characteristics and origin whereas Slatt and O'Brien (2011) discussed typical pore types in shale. Recent studies (e.g., Loucks and Reeds; 2014; Milliken and Curtis, 2016) revealed the differences between organic pores in depositional organic matter (detrital) and migrated organic matter (authigenic). Pore classification in material science based on physical adsorption and capillary condensation is also available (Chalmers et al., 2012).

For convenience of discussion in this study, we refer to matrix porosity as all non-organic porosities in the rock mineral matrix, such as inter- and intra-particle porosities (Loucks et al., 2012). The fracture porosity is also included in the matrix porosity. Organic pores may exist in different types of organic matter (Loucks et al., 2009; Bernard et al., 2012; Bernard and Horsfield, 2014; Loucks and Reeds, 2014; Reeds et al., 2014; Milliken and Curtis, 2016). The use of organic porosity in this study is restricted to the porosity that occurs within the original organic matter (depositional-organic-matter according to Loucks and Reeds; 2014) as a result of hydrocarbon generation. Crack formed by kerogen shrinkage due to loss of mass during hydrocarbon generation is also counted as organic porosity. Secondary organic pores, occurring within solid pyro-bitumen hosted in matrix pores or fractures, which is formed by thermal

cracking of migrated hydrocarbon liquid phases, does not create additional pore space. Rather, precipitation of pyro-bitumen reduces primary matrix porosity, similar to mineral precipitation in diagenesis (Wood et al., 2015).

In a tight-shale reservoir system, the matrix and organic pore systems have remarkable differences in physical and chemical characteristics, such as water/oil wettability (Passey et al., 2010; Li, 2013; Wang et al., 2013; Williams, 2013), pore size distribution (Loucks et al., 2009; Rine et al., 2011; Chalmers et al., 2012), natural gas adsorption capacity (Ross et al., 2009; Akkutlu and Fathi, 2012; Ambrose et al., 2012; Bohacs et al., 2013), gas transport characteristics and fluid thermodynamics (Akkutlu and Fathi, 2012). The size of matrix pores is predominantly in the order of the micrometre although nano-pores exist as crystal defects and intercrystal spaces in clay minerals (Milliken and Curtis, 2016); as a general rule primary pore diameter and volume decrease with increasing burial depth (Figure 1). The matrix pore is saturated with water when sediments are deposited and likely remains water wet (e.g., Wang et al., 2013). Conventional evaluation methods for clastic reservoir are applicable to estimating matrix pore system parameters such as porosity and water saturation.

In contrast, the organic pores are in the order of nanometre size, and the pore diameter and overall volume increase with maturation (burial depth) within the hydrocarbon generation windows (Figure 1). The abundance and type of organic matter are also critical elements to consider for that trend (Chalmers et al., 2009; Lu et al., 2015). Most interconnected organic pores are formed from the decomposition of kerogen during hydrocarbon generation. The organic matter is likely oil wet and no bound water exists in the organic pore system (Passey et al., 2010; Williams, 2013). In addition, because of the nano-scale of the pore system, fluid thermodynamics (phase behavior) differ from that in conventional reservoirs. A significant portion of organic pore space is filled with a adsorbed phase (Akkutlu and Fathi, 2012; Ambrose et al., 2012; Wang, et al., 2015; Wang et al., 2016). Detailed works showed that methane sorption increases with increasing Total Organic Carbon (TOC), indicating that organic matter is the primary control on methane sorption (Ross and Bustin, 2009; Chalmers et al., 2012; Zhang et al., 2012; Lu et al., 2015; Yu et al., 2015). The percentage of adsorbed phase in organic pores depends on the size of the nano-pores, and likely relates to the abundance, type and maturity of kerogen. Differing from conventional reservoirs, gas transport may be subject to slip flow, transition regime, or Knudsen diffusion depending on pore size, pressure and temperature (Akkutlu and Fathi, 2012, Williams, 2013).

The matrix porosity decreases with burial depth as a result of mechanical compaction and cementation. Mineral composition, grain size, texture of the sedimentary rock, compaction and diagenetic histories are

primary factors affecting matrix porosity (Ramm, 1991; Dutton and Loucks, 2010; Hammer et al., 2010; Bjørlykke and Jahren, 2012; Pommer and Milliken, 2015; Milliken and Curtis, 2016). Development of matrix porosity shows a remarkable change at a depth around 2500 metres, above which the decrease in rate in porosity is rapid and the primary control is mechanical compaction. Below that depth the porosity loss becomes slower and diagenetic processes (cementation) plays a more important role. A tight reservoir usually has a negative correlation between porosity and TOC (e.g., Montney on Figure 2a). This is because matrix pore dominates in tight reservoir and higher TOC values in a tight reservoir suggest the presence of higher fine-grained sediments content that will result in intervals with more compaction and reduction of both overall pore size and total pore volume.

In contrast, organic porosity increases with thermal maturity within hydrocarbon generation windows. The abundance and size of organic pores are a function of thermal maturity and TOC richness (Chalmers et al., 2009; Ross and Bustin, 2009; Jarvie, 2012a and b; Bernard et al., 2013; Curtis, 2013; Lu et al., 2015; Pommer and Milliken, 2015; Chen and Jiang, 2016). Due to distinct kerogen kinetics, thermal decomposition of one type of kerogen may differ from the others, resulting in variations in organic porosity, pore size distribution and characteristics at a given thermal maturation level (Loucks et al., 2009; Bernard et al., 2012; Bernard and Horsfield, 2014; Reeds et al., 2014; Lu et al., 2015; Chen and Jiang, 2016. Most organic pores form from thermal conversion of kerogen to hydrocarbons and no significant organic porosity is generated before the onset of oil generation. Organic porosity approaches a maximum when all convertible carbon has been converted to hydrocarbons. Thermal cracking of oil to gas in source rock reservoir may reverse the increasing trend of organic porosity as a result of pyro-bitumen precipitation. In general, self-sourced reservoirs exhibit positive relationships between TOC and organic porosity (Figure 2a) and a negative correlation between TOC and water saturation (Figure 2b). This is because TOC-rich source rocks have greater hydrocarbon generation potentials and can create more organic pores that are saturated with hydrocarbons rather than water due to their hydrophobicity.

Dual Porosity Model

The herein proposed method is a reservoir volumetric approach with a dual-porosity model that quantifies the reservoir storage for oil and gas. The method is designed for resource assessment in a tight-shale resource play, in which both the matrix porosity and organic porosity provide effective storage. Figure 3 illustrates the different components that have been incorporated to derive the volumetric equations for the calculation of oil and gas volumes.

The dual-porosity model takes into account three different storage mechanisms (Figure 3) in a tight-shale reservoir system: a) matrix pores (including natural fracture) with free hydrocarbon, and free and bound water; b) organic pores with free hydrocarbons; and c) organic pores with adsorbed hydrocarbons. The free hydrocarbon volume in the two different pore systems can be estimated from geochemical data and geophysical well logs. Additional laboratory tests are necessary to determine the adsorbed hydrocarbons. Figure 4 is a workflow chart showing the processes and steps for the estimation of hydrocarbon pore-volumes under the dual-porosity model. There are two parallel processes for the porosity calculation, hydrocarbon saturated matrix porosity using well log data and organic porosity estimations based on kerogen kinetics and mass balance. Because available geochemical data from core or cuttings samples for calculation of organic porosity are often limited by spatial coverage and vertical resolution, it is difficult to directly integrate the geochemical data with well log based matrix porosity calculation. In this study well log data are used to estimate TOC content using available methods such as the Passey method (Passey et al. 1990) or the revised Passey method (Chen et al., 2013, Wang et al., 2016), and Rock-Eval analytic results on core samples are used to calibrate the TOC calculations.

Organic porosity calculation

Various methods have been proposed for estimating organic porosity based on Rock-Eval or other types of data (e.g., Jarvie et al., 2007; Loucks et al., 2009; Modica and Lapierre, 2012; Kuchinskiy, 2013; Kohn et al., 2013; Romero-Sarmiento et al., 2013; Chen and Jiang, 2016). The proposed organic porosity calculation is based on that by Chen and Jiang (2016), which is a revised version of Modica and Lapierre (2012) with the improvement on reducing the impact of hydrocarbon expulsion on the initial/original TOC estimate. The evaluation of organic porosity includes the following steps: 1) generation of a kerogen decomposition model (which includes the development of a thermal maturation model and an estimation of hydrocarbon transformation ratio); 2) estimation of initial total organic carbon content (iTOC); and 3) calculation of organic porosity. The derivation and application examples are provided in Chen and Jiang (2016).

The organic porosity $\emptyset_{org}$ is estimated from the following equation:

$$\emptyset_{org} = \gamma[C_{toc}^{o}\alpha f T_R\left(1-\frac{0.833C_{toc}}{100}\right)]\frac{\rho_b}{\rho_k} \qquad (1)$$

where C_{toc} is the measured total organic carbon content (in weight fraction), α ($\alpha = H_i^o/1200$) is the percentage of petroleum convertible carbon in TOC (a function of kerogen type); f is an expulsion efficiency (fraction); T_R is transformation ratio that is a function of kerogen type and thermal maturity;

$\rho_b and\ \rho_k$ are the rock bulk density and the density of the kerogen respectively; and γ represents the carbon equivalent mass of kerogen in hydrocarbon conversion (γ=1.200).

The evolution of organic porosity is a theme less well understood and much improvement can be made in methodologies for estimating organic porosity. In Eq. (1), the effect of thermal cracking of oil to gas and precipitation of pyro-bitumen as suggested by Barker (1995) and Tian et al. (2008) in conventional reservoirs and by Wood et al. (2015) for tight reservoirs was not considered for two reasons. First, pyro-bitumen precipitation in source rock is different from that in reservoir. Oil cracking to gas takes place in high maturity when a large amount of oil has already been expelled from the source rock. Depending up on the expulsion efficiency (can be up to 85%), kerogen type and mineralogy, the subsequent precipitation of pyro-bitumen within source rock beds varies, but should be small. For a moderate expulsion efficiency of 70%, a mass balance calculation indicates a maximum of 15% reduction of the peak organic porosity through pyro-bitumen precipitation. Those hydrocarbons that remain in source rock, but reside in matrix pores outside of kerogen network, can further reduce the amount of carbon precipitation in organic pores. If additional hydrogen from water and minerals in the source rock system is available for hydrocarbon generation, the amount of pyro-bitumen can be significantly reduced (Seewald, 2003). Secondly, identification of the origins of various bitumen and organic pores can be difficult with the present available methods (Bernard and Horsfield, 2014; Loucks and Reeds, 2014). Thus comprehensive studies are needed to quantify the relationship between thermal oil cracking and pyro-bitumen precipitation in source rock reservoir with different kerogens that have distinct composition and molecular structures and kinetics, prior to development of a quantitative method for organic porosity reduction as a function of pry-bitumen precipitation.

Modeling of organic matter connectivity in source rock suggests that when kerogen is in excess of 7 wt%, it may form a 3D network, which could be subject to compaction (Kuo et al., 1995). It has also been reported that mineralogy of the source rocks may play an important role in organic porosity preservation (Fishman et al., 2012). Shales with high quartz and carbonate contents appear to be more resistant to the collapse of organic pores from burial compaction as well as to hydrocarbon generation and expulsion compared with shales with high content of clay mineral. In fact, mechanical compaction dominates in burial depth less than 2500 m (Figure 1) in most of basins, where massive hydrocarbon generation starts at greater depth in general. At depths greater than 2500 m, chemical compaction (diagenesis) will dominate. This can be seen, for example, from the shale compaction curve in Figure 1, which was constructed based on sonic transient times of the Devonian Duvernay Shale from more than 200

exploration wells across the Western Canada Sedimentary Basin. For a 3D kerogen network consisting of various organic pores and fractures, we argue that it is only when the diameter of the organic pore in the source rock is greater than the size of supporting mineral grain, the mechanic compaction could significantly affect the organic pores. However, studies show that organic pores are usually smaller than 100 nm (e.g., Loucks et al., 2009; Romero-Sarmiento et al., 2014; Chen and Jiang, 2016), smaller than the average size of a typical clay mineral. Overpressure from oil cracking to gas may provide additional support for the organic pores.

Adsorbed Gas Calculation

Langmuir (monolayer) gas absorption in organic rich shales can be described by the following Langmuir equations (Yu et al., 2015; Zhang, 2012):

$$V_P = V_L \frac{P_{res}}{P_L + P_{res}} \tag{2}$$

or

$$V_P = V_L \frac{KP_{res}}{1 + KP_{res}} \tag{3}$$

where V_L is the Langmuir volume (maximum capacity of adsorption), V_P is a specific adsorption capacity at reservoir pressure P_{res} (kPa), P_L is the Langmuir pressure (kPa), at which one half of the Langmuir volume (V_L/2) can be adsorbed; and K is the Langmuir constant (1/kPa) defined as

$$K = \exp\left(\frac{q}{RT} + \frac{\Delta s^0}{R}\right) \tag{4}$$

where q = Ea–Ed is the isosteric heat of adsorption, and Δs^0 is the standard entropy of adsorption (Zhang, 2012). By combining Eqs. (2), (3) and (4), one can obtain:

$$\ln(1/P_L) = \frac{q}{RT} + \frac{\Delta s^0}{R} \tag{5}$$

Eq. (5) demonstrates the dependency of P_L on temperature with a positive correlation between P_L and temperature.

Laboratory experiments indicate that the Langmuir volume can be affected by many factors, such as clay mineral, temperature, pressure, thermal maturity, water/moisture content and kerogen types (e.g., Hildenbrand et al., 2006; Zhang et al., 2012; Liu et al., 2013; Rexer, et al., 2013; Yu, et al., 2015). While attempt has been made to quantify the relative contributions from those factors using a multivariate regression (Hildenbrand et al., 2006), laboratory data often show that a simple correlation between TOC and V_L explains most of the variance in the data (e.g., Ross and Bustin, 2009; Jarvie, 2012b; Zhang, 2012; Yu et al., 2015; Gao et al., 2016), suggesting that organic richness is the primary control in shale gas

reservoir. Other variables such as temperature, pressure and thermal maturity are all systematically correlated and can be compensated by each other as indicated by theoretical (e.g., Eq. 5), or experimental relationships. For example, if we find the corresponding depths on each of the V_L curves with different vitrinite reflectance values and mark all the depths on the plot of sorption capacity and depth by different maturities (Fig 10 of Hildenbrand et al., 2006), one will find that all the marked points follow almost a straight vertical line. This is because the gain in sorption capacity due to increased pressure and maturity is a trade-off with increased temperature with burial depth. Studies indicate that water/moisture can substantially reduce the adsorption capacity of shale by pre-occupying the pore-surface (Joubert et al. 1975; Bustin and Clarkson, 1998; Zhang, et al., 2012; Liu et al., 2013). Sediments are water-saturated when deposited and water forms an irreducible film on the surface of matrix grains (including clay minerals) when hydrocarbon fluids migrate through, thus reducing the adsorption capacity by restricting the access to active sites on the surface.

The adsorbed gas forming a monolayer on internal surface area of shale by surface force can be estimated from the following equation (e.g., Ambrose et al., 2012):

$$Gas_{in-place}^{adsorbed} = V_{rock}\rho_b V_L \frac{P_{resv}}{P_L + P_{resv}} \tag{6}$$

where V_{rock} is the rock volume (m^3), ρ_b is bulk rock density (ton/m^3); P_{resv}: reservoir pressure (kPa); V_L: Langmuir volume (scf/ton), which can be approximated by a function of TOC content and is derived from the following relationship in this study:

$$V_L = \beta\, C_{toc} + C \tag{7}$$

where β is an unknown scale parameter, and C is a constant that relates to other contributions for the adsorbed methane in the reservoir. Both parameters can be determined from laboratory tests on rock examples, and Yu et al. (2015) provides a good example of obtaining such a relationship. It is noteworthy that the sorption capacity is the maximum gas that can be adsorbed, but not the quantity that the shale has actually adsorbed. As shale gas reservoirs are self-sourced systems, thermogenic gas is available to the shales in the gas generation window. Gasparik et al, (2012) reported that there is no correlation between sorption capacity and TOC for their black shale samples in the Netherland. In this case, one may take β=0 and an overall average of methane sorption capacity for C in Equation (7), or seek an alternative quantitative expression for quantifying methane sorption capacity.

Ambrose et al. (2012) indicated that adding the adsorbed gas from Eq. (6) directly could over-estimate the total gas in shale reservoir due to double counting as this part of pore space has already been considered in calculation of hydrocarbon pore volume. The over-estimation (in scf/ton) can be quantified by the following equation:

$$Gas_{ov}^{ad} = \frac{32.0368}{B_g}\left\{\frac{0.000001318\hat{M}}{\rho_s} V_L \frac{P_{resv}}{P_L + P_{resv}}\right\} \quad (8)$$

where $\hat{M}$is natural gas apparent molecular weight (16 lb/lb-mole), ρ_s is gas density in adsorbed-phase (0.34 g/cm^3) and *Bg* is gas formation volume factor. For details of the derivation of Eq. (8) and application examples, readers are referred to Ambrose et al. (2012). Yu et al. (2015) presented a mathematical formulation for estimating adsorbed gas considering multi-layers adsorption based on the BET isotherm. Application examples from Marcellus Shale suggest a slight increase in the amount of adsorbed gas as compared to those from the Langmuir monolayer isotherm model.

Hydrocarbon volumetric calculation

To capture the spatial variability of the resource potential in the target reservoir, the study area is divided into *N* equal sized cells with location index of *n*. The total hydrocarbon pore volume, V_{pHC}, in the reservoir can be estimated from the volumetric equation:

$$V_{pHC} = \sum_{n=1}^{N} A(n)T(n)\,\emptyset_{HC}(n) \quad (9)$$

where *A(n)* is the cell size (m^2), *T(n)* is the net reservoir thickness (m), $\emptyset_{HC}$ *(n)* is hydrocarbon saturated reservoir porosity (in fraction).

The following equations are used to convert the in-place oil and gas pore volumes in reservoir condition to in-place oil and gas volumes in standard surface condition.

$$V_{oil} = f_{oil}V_{pHC}/F_{VF} \quad (10)$$

$$V_{gas} = f_{gas}V_{pHC}/B_g \quad (11)$$

$$V_{gas}^{sol} = V_{oil}G_{OR} \quad (12)$$

where V_{gas}^{sol} is solution gas, F_{VF} is oil formation volume factor, *Bg* is gas formation volume factor and G_{OR} is gas to oil ratio.

Methods for conventional reservoir evaluation using well logs are applicable to the rock matrix porosity and hydrocarbon saturation calculations in unconventional systems. However, the discrimination of

organic porosity from effective porosity values based on well logs is still an area of active research. In this study, we assume that the well log porosity gives the total effective porosity, including the organic porosity as organic pores affect the density and sonic readings. More details of the reservoir parameter estimations are discussed in Chen et al. (2016).

Application to Utica Shale, Quebec

Geological Setting

In southern Quebec, a Cambrian – Upper Ordovician sedimentary rock succession is preserved in the St. Lawrence Platform (SLP) (Figure 5). At the base of the succession, the Middle Cambrian to lowermost Ordovician clastics of Potsdam Group unconformably overlies the Precambrian basement or is in faulted contact with the latter (Lowe and Arnott, 2016). Along the cratonic margin, the Lower Ordovician carbonate platform succession represented by intertidal to shallow subtidal limestones and dolostones of the Beekmantown Group was covered by a Middle to Upper Ordovician succession of initially slow to ultimately rapid deepening-upward foreland succession of limestone to argillaceous limestone (Chazy, Black River and Trenton groups) to black organic-rich mudstone (Utica Shale) and capped by shallowing-upward flysch and post-orogenic molasse (Lorraine and Queenston groups) (Lavoie, 2008). Based on detailed organic matter reflectance data, a minimum of 3 to 4 km of post-Queenston burial occurred (Bertrand, 1991) (Figure 6).

The Utica Shale consists of carbonate-rich mudstones and no sandy layers (Lavoie et al., 2008; Thériault, 2012a). The source of carbonate mud and its upsection abundance have been interpreted to be related to transgressive – regressive cycles with highstand shedding of mud from the platform which was backstepping onto the Precambrian craton at that time (Lavoie, 2008). Based on recent lithological, mineralogical and petrophysical data, Thériault (2012a, b) suggested the subdivision of the Utica Shale into two informal (lower and upper) members. The lower Utica is characterized by a mineralogical composition close to that of the underlying Trenton Group, whereas the mineralogy of the upper Utica reflects a progressive transition with the overlying Lorraine Group.

The Upper Ordovician Utica Shale has been, since the early days of hydrocarbon exploration in southern Quebec, considered as an excellent hydrocarbon source rock for conventional hydrocarbon systems (Lavoie et al., 2009). The paradigm shift towards its significance for unconventional resource play started in mid-2000 with initial drilling and testing of the Utica Shale. Thériault (2012a) has proposed three hydrocarbon fairways: a liquid rich zone, a condensate zone and a dry gas zone, for the Utica Shale in

southern Quebec (Figures 5 and 7). These zones are based on the depth (thermal alternation) of the Utica Shale as well as on structural domains (Thériault, 2012a; Lavoie et al., 2014). Shale gas exploration in the Utica Shale began in 2006 in southern Quebec. A total of 28 wells have been drilled (Figure 5), of which 18 wells have been hydraulically fractured until 2010. So far, the exploration has focused primarily on the central fairway, where 24 shale gas wells have been drilled. Based on a limited number of hydraulic fractures, initial production values were highly variable; the best IP value for a horizontal well was 11 mmscf/d of natural gas (Lavoie et al., 2014).

Data interpretation and models for resource assessment

Three types of data were compiled by Chen et al. (2014) and are used in this assessment: a) geological map and compiled data tables from the Ministère des Ressources Naturelles du Québec (Thériault, 2012a) that provide information on the spatial extent of the Utica Shale, its burial depth and thickness; b) geophysical well logs form from the Ministère des Ressources Naturelles du Québec; and c) geochemical data from Rock-Eval pyrolysis and thermal maturity indicators of source rocks compiled by Thériault (2012a and b) and some additional measurements from the Geological Survey of Canada (Lavoie et al., 2011; Haeri-Ardakani et al., 2015).

A total of forty eight exploration wells with digital gamma ray, caliper, sonic, porosity and resistivity logs were available to this study, forming an essential part of the dataset for volumetric calculation of resource potential. The geophysical well log data were used to estimate matrix and total porosities, and to calculate water saturation. The location of wells with digital petrophysical logs are shown in Figure 7. Another important dataset is the Rock-Eval pyrolysis results and vitrinite equivalent measurements of the Utica Shale. Analytical results from 946 samples in 79 wells and 23 outcrop locations are available to this study. Most of the samples from the 79 wells are cuttings. All the Rock-Eval data were generated using Vinci Technologies' Rock-Eval 6 instruments. There are many geological factors that could affect the quality of the Rock-Eval pyrolysis analysis. When TOC values are less than 0.5 wt%, pyrolysate adsorption on the mineral matrix can affect S1, S2 and Tmax values, an effect most significant for argillaceous rocks (Peters, 1986). In addition, Tmax values may not be reliable when S2 values are less than 0.2 mg HC/g rock, although this criterion likely varies depending on the type of organic matter and rock matrix. For example, Obermajer et al. (2007) suggested a minimum S2 value of 0.35 mg HC/g rock for correctly interpreting Tmax values based on data from the Arctic Islands. In addition to data quality, a challenge in this study is the mixture of source rock and non-source rock samples. The non-source rock samples are usually from tight reservoir, such as siltstone or carbonate layers interbedded with the

organic-rich shale or from coarser intervals within the Utica Shale. Haeri-Ardakani et al. (2015) showed organic petrological examples of the types of organic matter in different lithologies. The non-source rock samples contain no or little indigenous organic matter and the organic matter therein consists primarily of migrated hydrocarbon fluids and residual carbon that remain after oil has been cracked to gas in the deep burial realm. The Rock-Eval results from those samples usually exhibit low S2, high S1 and either extremely low or high Tmax values. To eliminate the effect of poor data quality and non-source rock samples on the analysis, the data were scrutinized carefully. Screening criteria of TOC > 0.5%, 520°C > T_{max} >400°C and S2 > 0.35 were applied to the original data and effort was also made to eliminate samples of possible contaminations from both drilling mud and migrated hydrocarbons (very high production index (PI=S1/(S1+S2)), but low maturity). This resulted in the removal of a large number of samples that were considered to be unreliable. The average TOC value of the remaining 223 measurements is 0.9% with highest observed value being 5.2% for Upper Ordovician shales in southern Quebec. Figure 8 presents various regional geological maps showing some of the major geological features of the Utica Shale in the study area.

Peters et al. (2006) suggested that kerogen types defined by hydrogen index from Rock-Eval analysis is not systematically related to kerogen kinetic responses and that default numerical kinetic models of hydrocarbon generation can introduce unacceptable errors. Therefore, an empirical approach based on a real dataset is taken in this study. Two empirical models are constructed for the hydrocarbon generation and bulk composition prediction. A hydrocarbon transformation ratio model based on hydrogen index and Tmax data is used to represent hydrocarbon generation. The bitumen index equivalent of Espitalié et al. (1987) along with hydrogen index derived from Rock-Eval pyrolysis data are used to determine the relative volumes of oil and gas in the pore volume.

Due to high thermal maturity and mixing of migrated hydrocarbons and in situ organic matter in different porous media of the samples, a plot of hydrogen index against T_{max} shows relatively large scattered clouds with predominantly high T_{max} values (Figure 9a). Because the majority of data points are from thermally mature and over mature samples, there is little information to evaluate the initial hydrogen index value of immature source rock. Organic petrology study shows that kerogen in the Utica Shale consists predominantly of marine-derived organic matter as suggested by the presence of chitinozoan and marine liptinite and liptodetrinite, though significant portion of the bulk organic matter is migrated pyro-bitumen (Haeri-Ardakani et al., 2015). To determine the kerogen kinetic properties and generation potential, we use the coeval, lower mature Collingwood Member of the Upper Ordovician Lindsay Formation (Ontario,

eastern Canada) (Macauley and Snowdon, 1984; Obermajer et al., 1999; Chen et al., 2016) as an analogue for the Utica Shale. Available thermally mature and early mature shale core samples from exploration wells cutting through the Collingwood Member in the foreland basin were analyzed and the data points are superimposed on the same plot to compare with the data from the Utica Shale. The two datasets (Utica and Collingwood in the Appalachian foreland basin) are complementary in thermal maturation coverage, with the Collingwood Member samples covering the marginally and moderately mature fields and the Utica Shale samples overlap the mature and over mature domains. The generation kinetics for the Utica evaluation were studied by analyzing the thermal decomposition behaviour as revealed by the decreasing trend of remaining hydrocarbon generation potential (indexed by HI) with increasing thermal maturity (indexed by Tmax) using the data-driven method by Chen and Jiang (2015). Based on the two shale data sets, an empirical model of the hydrogen index as a function of T_{max} is constructed (Chen and Jiang, 2015) (broken black line in Figure 9a). The data clouds around this empirical model represent the uncertainty in the data set, likely related to possible variations either in organic facies, mixing of indigenous and migrated organic matters or other factors (for example, Snowdon, 1995). A transformation ratio model is then built from the Espitalié et al. (1987) method using the established Tmax-HI model (Figure 9a). Figure 9b presents the estimated transformation ratio as a function of Tmax based on the empirical model in Figure 9a showing the onset of hydrocarbon generation at Tmax around 435°C with the end of hydrocarbon generation at T_{max} at around 480^{o}C.

There are a number of methods that can be used to estimate the bulk oil and gas volumes. Zhao et al. (2007) used a maturity index derived from Archie equation and related this index to gas to oil ratio; Kuhn et al. (2010) used basin/petroleum system tools to estimate bulk composition and phase behaviors in the Bakken Shale. The method used in this paper follows the idea of Justwan and Dahl (2005) and Pang et al., (2005). A plot of Bitumen Index Equivalent (BIE=S1/TOC*100, equivalent of bitumen index, BI, of Espitalié, et al., 1987) against T_{max}, is used to determine the onset of oil generation and thermal cracking of oil to natural gas (Figure 9c). The onset of thermal cracking of oil to natural gas from this model is indicated by the maximum BIE at Tmax around 450^{o}C. For the Utica Shale, this is coincident with the development of overpressures in the reservoir and δ^{13}C isotopic roll-over for gas as shown by Chatellier et al. (2013). The ratio of BIE and Hydrocarbon Generation Index (HGI=initial hydrogen index – present hydrogen index) represents the portion of bulk oil remaining in the tight-shale reservoir system, based on which oil and gas pore volumes in reservoir condition can be converted into the in-place oil and gas volumes at standard surface conditions by reservoir engineering equations (Eqs. 9, 10 and 11).

Studies by Chen et al. (2014) and Haeri-Ardakani et al. (2015) indicated that the Utica Shale is an unconventional resource play with mixed porous media consisting of matrix pores and organic pores. Petroleum originated from the organic-rich shale is stored within the stratigraphic intervals including the embedded tight limestone and silty mudstone reservoirs. The matrix porosity and natural fractures provide the principal storage medium for expelled petroleum and additional petroleum remains within organic pores in the source rock. For the convenience of this assessment, we treat the entire Utica Shale as a whole and assume it comprises stacked reservoirs with mixed porosities and forms a continuous tight-shale resource play. Hydrocarbon shows and flows from recent exploration wells indicate that all essential geological elements for forming oil and gas accumulations in this resource play are present, while the quantity of oil and gas in the Utica Shale is the subject for evaluation herein.

The calculation of hydrocarbon volume is based on individual exploration wells with adequate well log data (Figure 4). Well logs were used for calculation of matrix porosity and water saturation. All log models were calibrated by laboratory measurements prior to their use in the volumetric parameter evaluation. Oil, free gas, associated gas and adsorbed gas were assessed at each well and spatial geostatistical models (semivariogram models) derived from data were used to infer the spatial variation of the resources and to capture the uncertainty where data were extrapolated spatially. The uncertainties in spatial extrapolation and interpolation for each component (oil, free gas, associated gas and adsorbed gas) are expressed as variance maps. Monte Carlo methods were employed to aggregate hydrocarbon resources of each cell in the study area to form probabilistic distributions. The ranges of probabilistic distributions of oil and gas resources represent the uncertainties in the assessment.

Data analysis indicates that laboratory TOC measurements have a low vertical resolution and variability representation. A revised Passey model (Chen et al., 2013) was used to estimate TOC content at each log data points. Well logs were first calibrated by available TOC measurements from Rock-Eval analysis and used to establish the revised Passey model, from which TOC content was estimated at any given depth within the Utica Shale interval at all data well locations.

Prior to determining the intitial TOC, the expulstion efficiency factor (f) has to be assessed (Chen and Jiang, 2016). Well log TOC evaluation method provides only TOC estimates, other parameters such as Rock Eval S1 and S2 values are not available for calculation of the expulsion efficiency factor. Therefore, hydrogen index (Figure 9a) and bitumen index equivalent (Figure 9c) models are used to estimate the expulsion efficiency factor. Figure 9d compares the transformation ratio and expulsion efficiency models

as a function of thermal maturity index (Tmax). The estimated initial TOC contents were then used to estimate organic porosity following the relationship in Eq. (1).

The total hydrocarbon saturated porosity in Eq. (8) is the sum of hydrocarbon saturated matrix porosity and organic porosity, and the hydrocarbon pore volume is the sum of hydrocarbon saturated pore volumes in the identified potential pay zones within the Utica Shale at each well location. Figure 10a is a kriged map of the hydrocarbon pore volume of the Utica Shale showing the spatial variation of the estimated hydrocarbon pore volume across the basin. Geostatistical data analysis suggests a better continuity of hydrocarbon pore volume in the NE-SW direction. The estimated hydrocarbon pore volume was then separated into oil and gas pore volumes based on the empirical kinetic model of the source rock in the Utica Shale, and subsequently converted to oil and gas volumes respectively at standard surface conditions.

Assessment Results

The assessment resulted in four different in-place resources: oil, free-gas, dissolved gas and adsorbed gas. Three gas components are aggregated into total gas (Figures 10b to d). In the absence of significant production data, no attempt is made to estimate the technically recoverable portion of the in-place resources.

The estimated in-place oil resource is graphically shown as a statistical distribution in Figure 11 and numerically in Table 1, both presenting the range of uncertainty in the assessment. The estimated oil resource potential varies from 0.69 to 3.72 billion of barrels (Bbls) with a mean of 1.80 Bbls. This study also provides a resource density map (Figure 10b) to identify geographical locations of possible oil "sweet-spots" in the Utica Shale. The oil resource in the Utica Shale occurs primarily in the northwestern margin of the basin, where the source rock is still in the oil or condensate generation window (Figure 10b). This indicates that the burial depth and thermal maturity are the major control factors for oil resource in the Utica Shale in the St. Lawrence Platform.

Figure 12 displays the probability distribution of the estimated in-place natural gas resources showing the relative contributions from the free, adsorbed and dissolved gas. The estimated in-place resources for the three different types of gas are listed in Table 2. The free gas estimates vary from 47.44 to 163.34 TCF with a mean of 91.91 TCF (Figures 12a-b). The estimated adsorbed gas also shows considerable uncertainty ranging from 24.69 to 61.23 with a mean value of 40.52 TCF (Figures 12c-d and Table 2), about 1/4 of the total gas resource, which is considerably lower than other basins. For example in the

Barnett Shale, adsorbed gas is over half the total gas (Romero-Sarmiento et al., 2013). This is because the adsorbed gas is primarily controlled by the present day TOC content as indicated by Eq. (7) and the average TOC is only 0.9% in the Utica Shale in Quebec. The contribution from the solution gas is even smaller and the estimates vary from 19.98 to 51.05 TCF with a mean of 31.25 TCF (Figures 12e and f). The best estimate of the aggregated total natural gas resource (free, dissolved and adsorbed gases) in the Utica Shale in the St. Lawrence Platform is 164.07 TCF with a large uncertainty ranging from 101.50 TCF to 258.32 TCF (Figure 12g and h). Figure 13 shows the relative contributions of three gases and their uncertainty ranges as a composite probabilistic distribution plot.

The spatial variation of the solution gas is similar to that of the oil in place, while the adsorbed resource depends on the volume of organic matter in the formation (Eqs. 5 and 6). The spatial variation of the resource density of adsorbed gas is controlled by both the richness of TOC and the thickness of Utica Shale. The resource density is highest where TOC and formation thickness are high and thick in the southwest of the study area (Figure 10c). Figure 10d shows the geographic distribution of the aggregated total in-place natural gas resources. It appears that the largest accumulation occurs in the central and southern parts of the region in the condensate and dry gas zones as indicated by the thermal maturity (Figure 7). Similar to the hydrocarbon pore volume, the in-place sweet spots of high resource density area follow a northeast-southwest trend, which is parallel to the major trend of the foreland basin and to the orientation of present day maximum horizontal stress.

To compare the well log interpretation and the predicted spatial distribution of the resources, public domain well production test data (gas or oil) from the industry were collected from various sources. Twenty two oil and gas exploration wells in the period from 1970 to 2007 have been tested for oil and gas, among which seventeen wells show significant gas and oil flows. Since 2007, twenty-eight horizontal and vertical wells were drilled for the Utica Shale play, some of which were treated with hydraulic fracture stimulations. Although limited test and production results have been released for the horizontal wells (Marcil et al., 2012), successful gas and oil flows populate the areas or the trends with high estimated resource abundance (high hydrocarbon pore volume) indicated by this study, and this includes the best performing well (Talisman St. Edouard #1) with an initial natural gas production of 11 mmcf/d and a stabilized rate of close to 6 mmcf/d after 30 days. The geographical coicidence of two completely independent datasets suggest that the spatial variation of the resource abundance indicated by the hydrocarbon pore volume in this study likely reflects the general trend of resource potential in the Utica Shale (Figure 10d) in the St. Lawrence Platform.

The resource density maps and probabilistic distributions are constructed based on the kriged mean and variance maps of hydrocarbon pore volume, source rock kinetic properties and reservoir PVT (pressure, gas volume and temperature relationship) models, although, little is known about reservoir PVT. It is expected that there is a large uncertainty in the conversion from hydrocarbon pore volume to the standard surface volume that may not be captured in the resource volumetric calculations. As high thermal maturity makes the inference of the original status of the organic matter difficult, the initial source rock potential constitutes another major uncertainty. Because the majority of the Rock-Eval data from the Utica Shale are in the high and over-mature level, the kinetic model relies partly on the analogue immature to early mature samples from the coeval and facies-equivalent Upper Ordovician Collingwood Member in nearby southeastern Ontario (Macauley and Snowdon, 1984; Obermajer et al., 1999; Armstrong and Carter, 2010). The Utica and Collingwood shales share a similar tectono-stratigraphic setting being deposited on top of the foundering carbonate foreland ramp, although it is possible that subtle differences in depositional environment of the Collingwood Member of the Appalachian basin in southeastern Ontario from that of the Utica Shale in southern Quebec could lead to uncertainties in organic richness and kerogen kinetic behavior. These could in turn affect the predicted abundance and occurrence of oil and gas resources. However, the geographical distribution of predicted oil and gas resources from this study appear to be consistent with the maturity map (Figure 7), which suggests that the Collingwood Member is an appropriate analogue to the Utica Shale at least in terms of kerogen kinetics.

The expected in-place resources of 164 TCF of natural gas and 1.8 billion barrels of oil presented in this paper are slightly lower than previous in-place resource estimates of 183 TCF of natural gas and 2.3 billion barrels of oil reported in Chen et al. (2014). This is explained by the adoption of the revised method for organic porosity estimation. The study by Chen et al. (2014) used the method proposed by Modica and Lapierre (2012), which is based entirely on kerogen kinetics without considering mass balance due to hydrocarbon expulsion. We recognized that ignoring mass balance in the calculation may lead to a slightly overestimated organic porosity. The new approach with two mass balance corrections (Chen and Jiang, 2016) results in lower initial TOC and organic porosity and thus slightly lower resource estimates.

Discussion

Current available resource assessment methods in the public domain are either designed for evaluating resource potential in conventional reservoir without discriminating matrix porosity from organic porosity (e.g., Ambrose et al., 2012), or consider organic porosity only (e.g., Modica and Lapierre, 2012). Complex tight-shale reservoir systems with hydrocarbons filling both matrix and organic porosity cannot be satisfactorily evaluated with either approach alone. The new method is designed for assessing the unconventional resource potential in tight-shale reservoir systems with lithological characteristics in a transition between tight sandstone/siltstone to organic rich mudstone/shale (Passey et al., 2010; Williams, 2013). In such a reservoir system, laminations or alternations in lithology and texture are common features, and both the matrix porosity and organic porosity provide effective storage (Ambrose et al., 2012; Modica and Lapierre, 2012). The matrix porosity may provide the principal storage for expelled petroleum, whereas additional petroleum remains within organic pores in the source rocks. The proposed method is a reservoir volumetric approach with a dual-porosity model that quantifies different reservoir storages for oil and gas and is suitable for resource assessment in a tight-shale resource play.

The dual-porosity model takes into account three different storage mechanisms in a tight-shale reservoir system: a) matrix pores (including natural fractures) with free hydrocarbon, and free and bound water; b) organic pores (cracks in organic matter due to the loss of mass during hydrocarbon generation are also included) with free hydrocarbons; and c) organic pores with adsorbed hydrocarbons. The free hydrocarbon volume in the two different pore systems can be estimated from geochemical data and geophysical well logs separately. This new method is flexible and can assess hydrocarbon resources in the two end member reservoirs. When the reservoir is completely tight, where organic pores becomes irrelevant, the proposed method becomes a traditional reservoir volumetric approach and uses petrophysical data to estimate the reservoir volumetric parameters; whereas for a pure shale reservoir, where the organic pores dominate, the proposed method can approximate the hydrocarbon resource potential by estimating the organic pore volume, like the example shown for the Mowry Shale in the Powder River Basin of Wyoming by Modica and Lapierre (2012)..

The matrix and organic pore systems have major differences in physical and chemical characteristics, such as water/oil wettability, pore size distribution, natural gas adsorption capacity, gas transport characteristics and fluid thermodynamics (Passey, et al., 2012; Loucks, et al. 2009; Chalmers,et al., 2012; Ambrose et al. 2010; Akkutlu and Fathi, 2012). Identifying the storage type and quantifying the amount of resources in each type of pore systems provide additional information for resource development

planning as hydrocarbons in different storages with distinct characteristics require unique recovery techniques or special treatments for improved productivity and recovery.

The dual-porosity model for resource assessment relies on an existing method for estimating organic porosity (Modica and Lapierre, 2012; Chen and Jiang, 2016). Characterizing organic hosted pororosity is an emerging area that requires better understanding of the origin and evolution of the organic matter. Formation of organic pores in source rocks involves many factors, various intermediate products and interactions that complicate the processes (Loucks, 2009; 2012; Bernard, et al., 2012). There are uncertainties or questions and even disputes on how much of the intermediate products, such as pyro-bitumen, affect the pore size and initial organic porosity, and if the organic pores in a kerogen network can survive continued mechanical compaction at a depth range for commercial hydrocarbon production (Reed, et al., 2014; Bernard and Horsfield, 2014; Fishman, et al., 2012). Improvement of the organic porosity prediction requires quantification of the changes in the pore space within the network of organic matter as a function of thermal maturity, type of kerogen, mineral and formation water composition and burial depth. These remain as open questions and require future study.

Resource assessment helps to infer the unknown quantity and characteristics of hydrocarbons residing in subsurface using our knowledge and analogues obtained from where large amount of data are available and the hosting sedimentary rocks have been studied thoroughly. Resulting estimates are inherently imprecise due to uncertainties in our geological knowledge and inadequacy in data for inferring the resources. Attempts have been made to estimate and manage the uncertainty by using geostatistic tools for quantifying the uncertainty where spatial extrapolation was made and by using Monte Carlo simulation in calculation and aggregation of the resources to measure the propagation of uncertainty. The ultimate uncertainties of the resource estimates are represented by probability distributions for each resource categories and the total potential. The resulting distributions of the resource estimates suggest large range of uncertainty. Finding the major contributors for the uncertainty and reducing uncertainty remains a subject for future study.

Conclusions

We proposed a dual-porosity model to handle the complexity of mixed pore systems in assessing hydrocarbon resource potential in unconventional tight-shale reservoir systems. The proposed method treats the two distinct pore systems separately and estimates their properties based on various sources of

data, so that petroleum fluids in the two pore systems can be better characterized and assessed based on our current understanding of the unconventional tight-shale reservoir. The new method has the flexibility of assessing resource potentials for the entire spectrum of mixed lithology reservoirs from tight (fine-grained sandstone and siltstone) to source rock (organic–rich shale/mudstone). It can provide additional information regarding the dominant type of pore medium and the amount of resource in each of the pore systems, which are potentially useful for resource development planning aimed at improving productivity and recovery.

Our work suggests that the Utica Shale of the St. Lawrence Platform in southern Quebec of Canada is a tight-shale resource play with mixed reservoirs. The matrix porosity and natural fractures host migrated hydrocarbons, while organic pores contain the remaining *in situ* hydrocarbons thermally generated from the *in situ* kerogen in the shale. The proposed dual porosity model has been applied to the Utica Shale to illustrate the new resource evaluation method. The volumetric calculations indicate that the Utica Shale in southern Quebec contains large volumes of hydrocarbon resources with expected in-place resources of 164 TCF of natural gas and 1.8 billion barrels of oil. This study also generated resource density maps to outline potential in-place sweet spots with high resource abundance, providing additional information that may be useful for various decision making. The results of the application suggest that the proposed approach handles the two pore systems in a tight-shale reservoir well and provides a useful tool for estimating resource potential in an unconventional play with mixed porosity systems.

Acknowledgements

The authors are grateful to Robert Thériault of the Ministère des Ressources Naturelles et de l'Énergie du Québec for discussions and access to Québec's government Utica Shale data. Talisman Energy Incorporated is thanked for access to laboratory core test results. Useful comments and suggestions from internal reviewer Dr. Nicolas Pinet of Geological Survey of Canada and graphical assistance from Christine Deblonde are appreciated. Associate editor Prof. A. Aplin and two anonymous journal reviewers are thanked for their constructive comments and suggestions. ESS contribution # 20140328.

References

Akkutlu, I.Y. and Fathi, E. 2012. Multiscale gas transport in shales with local kerogen herogeneties: SPE Journal, December, p.1002-1011.

Ambrose R.J., Hartman, R.C., Diaz-Campos, M. Akkutlu I. Y. and Sondergeld, C. H. 2012. Shale gas-in place calculations Part I: New pore-scale considerations: SPE Journal, March, p. 219-229.

Aplin, A. C. and Macquaker, H. S. J. 2011, Mudstone diversity: Origin and implications for source, seal, and reservoir properties in petroleum systems: AAPG Bulletin, v. 95, p. 2031–2059.

Armstrong, D.K., and Carter, T.R., 2010. The subsurface Paleozoic stratigraphy of southern Ontario: Ontario Geological Survey, Special v.7, 301 p.

Barker, C., 1990, Calculated volume and pressure changes during the thermal cracking of oil to gas in reservoirs: AAPG Bulletin, v. 74, p. 1254-1261.

Bernard, S. and Horsfield, B. 2014. Reply to comment on "Formation of nanoporous pyrobitumen residues during maturation of the Barnett Shale (Fort Worth Basin)": International Journal of Coal Geology, v. 127, p.114–115.

Bernard, S., R. Wirth, Schreiber, A., Schulz, H-M. and Horsfield, B. 2012. Formation of nanoporous pyrobitumen residues during maturation of the Barnett Shale (Fort Worth Basin): International Journal of Coal Geology v.103, p.3–11.

Bertrand, R., 1991. Maturation thermique des roches mères dans les bassins des basses-terres du Saint-Laurent et dans quelques buttes témoins au sud-est du Bouclier canadien: International Journal of Coal Geology, v. 19, p.359-383.

Bjørlykke, K. and Jahren, J. 2012. Open or closed geochemical systems during diagenesis in sedimentary basins: Constraints on mass transfer during diagenesis and the prediction of porosity in sandstone and carbonate reservoirs: AAPG Bulletin, v. 96, p. 2193–2214

Bohacs, K.M., Passey, Q. R. Rudnicki, M., Esch W. L. and Lazar, O. R. 2013, The spectrum of fine-grained reservoirs from "shale gas" to "shale oil/tight liquids: Essential attributes, key controls, practical characterization: IPTC 16676, 16 p.

Bordenave, M. L., Espitalié, J., P. Leplat, J. L. Oudin, L. and Vandenbroucke, M. 1993. Screening techniques for source rock evaluation, *in* M. L. Bordenave, ed., Applied petroleum geochemistry: Paris, France, Editions Technip, p. 217–278.

Chalmers, G. R. L., and Bustin, R. M. 2008. Lower Cretaceous gas shales in northeastern British Columbia: Part I. Geological controls on methane sorption capacity: Bulletin of Canadian Petroleum Geology, v. 56, p. 1–21.

Chalmers, G., Bustin R. M. and Power, I. M. 2012. Characterization of gas shale pore systems by porosimetry, pycnometry, surface area, and field emission scanning electron microscopy /transmission electron microscopy image analyses: Examples from the Barnett, Woodford, Haynesville, Marcellus, and Doig units: AAPG Bulletin, v. 96, p. 1099–1119.

Chatellier, J., K. Ferworn, N. L. Larsen, S. Ko, P. Flek, M. Molgat and I. Anderson, 2013. Overpressure in shale gas: when geochemistry and reservoir engineering data meet and agree, *in* J. Chatellier and D. Jarvie, eds., Critical assessment of shale resource plays: AAPG Memoir 103, p. 45–69.

Chen, Z.; Liu, Y. Osadetz, K. Xu, B., Hu, K. and Guo, Q., 2013. A revised ΔlogRt method for shale play resource potential evaluation, - An example from Devonian Duvernay Formation, Western Canada Sedimentary Basin (abstract), 15th Annual conference of the International Association for Mathematic Geosciences, Madrid, Spain, September 2-6, 2013.

Chen, Z., Lavoie, D. and Malo, M. 2014, Geological Characteristics and Petroleum Resource Assessment of Utica Shale, Quebec, Canada: Geological Survey of Canada, Open File 7606, 43 p. doi:10.4095/293793

Chen, Z. and Jiang, C. 2015. A Data Driven Model for Studying Kerogen Kinetics with Application Examples from Canadian Sedimentary Basins, Marine and Petroleum Geology, V. 67, p.795-803, doi:10.1016/j.marpetgeo.2015.07.004.

Chen, Z., Jiang, C. Chen, C., 2015. Comparison of Source Rock Kerogen Kinetics Using a Data-Driven Model and Based on Rock-Eval Pyrolysis Data. AAPG ICE, Melbourne Australia, Sept. 13-16, 2015. http://ice.aapg.org/2015/program/monday-oral.

Chen. Z., Osadetz, K.G., Chen, X., 2015, Economic appraisal of shale gas resources, an example from the Horn River shale gas play, Canada. Petroleum Geoscience, (2015) v. 12., p.712–725. doi: 10.1007/s12182-015-0050-9.

Chen, Z. and Hannigan, P., 2016, A Shale Gas Resource Potential Assessment of Devonian Horn River Strata Using a Well-Performance Method, *Canadian Journal of Earth Sciences*, 2016, v.53, p.156-167, doi: 10.1139/cjes-2015-0094.

Chen, Z., Jiang, C., Lavoie, D. and Reyes, J., 2016. Model-Assisted Rock-Eval Data Interpretation for Source Rock Evaluation: Examples from Producing and Potential Shale Gas Resource Plays, International Journal of Coal Geology. v. 165, p. 290–302.

Chen, Z. and Jiang, C., 2016. A revised method for organic porosity estimation using Rock-Eval pyrolysis data, example from Duvernay Shale in the Western Canada Sedimentary Basin, AAPG Bulletin, V. 100, pp.405-422. DOI:10.1306/08261514173.

Chen, Z., Lavoie, D., Jiang, C., Duchesne, M.J., and Malo, M., 2016. Geological Characteristics and Petroleum Resource Assessment of the Macasty Formation, Anticosti Island, Quebec, Canada; Geological Survey of Canada, Open File 8018, 67 p. doi:10.4095/297865. http://geoscan.nrcan.gc.ca/starweb/geoscan/servlet.starweb?path=geoscan/downloade.web&search1=R=297865

Cooles, G. P., Mackenzie A. S. and Quigley, T. M. 1986. Calculation of petroleum masses generated and expelled from source Rocks: Organic Geochemistry,. V. 10, p. 235-245.

Curtis, M.E., Cardott, B. J. Sondergeld C. H. and Rai, C. S. 2012. Development of organic porosity in the Woodford Shale with increasing thermal maturity: International Journal of Coal Geology v.103, p.26–31

Curtis, M. E. 2013. Influence of Thermal Maturity on Organic Shale Microstructure; Oklahoma Shale Gas and Oil Workshop, November 20, 2013. Last access: June 12, 2014. http://www.ogs.ou.edu/MEETINGS/Presentations/2013Shale/2013ShaleCurtis.pdf

CSUG, 2010, Understanding shale gas in Canada, <accessed on Sept. 4, 2014> http://www.csur.com/sites/default/files/shale_gas_English_Web.pdf

Dutton S.P., and Loucks, R. G. 2010. Diagenetic controls on evolution of porosity and permeability in lower Tertiary Wilcox sandstones from shallow to ultra-deep (200-6700) burial, Gulf of Mexico Basin, USA: Marine and Petroleum Geology, v.27 p.69-81.

EIA, 2013. Shale gas and shale oil resource assessment methodology in EIA/ARI world shale gas and shale oil resource assessment. http://www.adv-res.com/pdf/00_EIA_ARI_Study_Methodology%20June_2013_FINAL.pdf. (Last access October 2014) .

Eseme, E., 2006. Oil shales: Compaction, Petroleum Generation and Expulsion. Ph. D Dissertation, Aachen University. http://darwin.bth.rwth-aachen.de/opus/volltexte/2006/1601/pdf/Eseme_Emmanuel.pdf

Eseme, E., Littke, R., Krooss, B.M., Schwarbauer, J., 2006. Experimental investigation of the compositional variation of acyclic paraffins during expulsion from source rocks: Journal Geochemical Exploration v. 89, p.100-103.

Espitalié, J., F. Marquis, L. Sage, and I. Barsony, 1987. Géochimie organique du bassin de Paris : Revue de l'Institut Français du Pétrole, v. 42, p. 271–302.

Fishman, N.S., H. A. Lowers, P. C., Hackley, R. J., Hill and S. O. Egenhoff, 2012. Porosity in Shales of the Organic-Rich Kimmeridge Clay Formation (Upper Jurassic), Offshore United Kingdom, Search and Discovery Article #50620 (2012), Posted June 25, 2012. http://www.searchanddiscovery.com/documents/2012/50620fishman/ndx_fishman.pdf.

Gao, X., Liu, L., Jiang, F., Wang Y., Xiao, F., Ren, Z., and Xiao, Z., 2016, Analysis of geological effects on methane adsorption capacity of continental shale: a case study of the Jurassic shale in the Tarim Basin, northwestern China, Geological Journal, v.51: p.936–948.

Gasparik, M., Ghanizadeh, A., Bertier, P., Gensterblum, P. Bouw, S. and Krooss, B. M., 2012, High-Pressure Methane Sorption Isotherms of Black Shales from The Netherlands. Energy Fuels, v.26, p. 4995−5004. dx.doi.org/10.1021/ef300405g.

Haeri-Ardakani, O., Sanei, H., Lavoie, D., Chen Z. and Jiang, C. 2015. Geochemical and petrographic characterization of the Upper Ordovician Utica Shale, southeastern Quebec, Canada: International Journal of Coal Geology, v. 138, p. 83-94. DOI: 10.1016/j.coal.2014.12.006

Hammer, E., Mørk M. B. E. and Næss, A. 2010,. Facies controls on the distribution of diagenesis and compaction in fluvial-deltaic deposits: Marine and petroleum geology, v. 27, p. 1737–1751.

Hildenbrand A., Krooss, B.M., Busch A. and Gaschnitz R., 2006. Evolution of methane sorption capacity of coal seams as a function of burial history - a case study from the Campine Basin, NE Belgium. International Journal of Coal Geology, v. 66, p.170-203.

Hill, R., Zhang, E. , Katz, B. J. and Tang, Y., 2006. Modeling of gas generation from the Barnett Shale, Fort-Worth Basin, Texas: AAPG Bulletin, v. 91, p. 501-521.

Jarvie, D.M., Hill, R., Ruble T. E. and Pollastro, R. M., 2007. Unconventional shale gas system: the Mississippian Barnett shale of north-central Texas as one model for thermogenic shale gas assessment: AAPG Bulletin, v. 91, p.475-499.

Jarvie, D. M., and Lundell, L. L. 2001. Amount, type, and kinetics of thermal transformation of organic matter in the Miocene Monterey Formation, *in* C. M. Isaacs and J. Rullkotter, eds., The Monterey Formation: From rocks to molecules: New York, Columbia University Press, chapter 15, p. 268– 295.

Jarvie, D. M., 2012a. Shale resource systems for oil and gas: Part 2—Shale-oil resource systems, *in* J. A. Breyer, ed., Shale reservoirs—Giant resources for the 21st century: AAPG Memoir 97, p. 89–119.

Jarvie, D. M., 2012b. Shale resource systems for oil and gas: Part 1—Shale-gas resource systems, *in* J. A. Breyer, ed., Shale reservoirs—Giant resources for the 21st century: AAPG Memoir 97, p. 69–87.

Jiang, C., Chen, Z. Mort, A. Milovic, M. Robinson, R. Stewart, R. and Lavoie, D., 2016. Hydrocarbon evaporative loss from shale core samples as revealed by Rock-Eval and thermal desorption-gas chromatography analysis: Its geochemical and geological implications, Marine and Petroleum Geology.. v.70, p. 294-303, http://dx.doi.org/10.1016/j.marpetgeo.2015.11.021

Joubert, J. I., Grein, C. T. and Bienstock, D., 1975. Effect of Moisture on the Methane Capacity of American Coals. Fuel 1974 Jul; v. 53. p.186-191.

Justwan, H. and Dahl, B. 2005. Quantitative hydrocarbon potential mapping and organofacies study in the Greater Balder area, Norwegian North Sea, *in* Dore, AG. and A. Vinino, eds, Petroleum Geology, Northwest Europe and global prospective – Proceedings of the 6th Petroleum Geology Conference, p.1317-1329.

Kuchinskiy, V. 2013. Organic Porosity Study: Porosity Development within Organic Matter of the Lower Silurian and Ordovician Source Rocks of the Poland Shale Gas Trend, Search and Discovery Article #10522. http://www.searchanddiscovery.com/documents/2013/10522kuchinskiy/ndx_kuchinskiy.pdf

Kuhn, P. P., 2013. Integrated Geochemistry and Basin Modeling Study of the Bakken Formation, Williston Basin, Ph.D Thesis, University of Berlin, p.241.

Kuhn, P. P., di Primio, R. Hill, R., Lawrence J. R. and Horsfield, B. 2012. Three-dimensional modeling study of the low-permeability petroleum system of the Bakken Formation: AAPG Bulletin, v. 96, p. 1867-1897.

Kuo, L. Hardy, H.H. and Owili-Eger, A.S.C., 1995. Quantitative modeling of organic matter connectivity in source rocks using fractal geostatistical analysis. Organic Geochemistry, v.23, p.29-42.

Lavoie, D., Obermajer, M. and Fowler, M.G. 2011. Rock-Eval/TOC data from Cambrian-Ordovician St. Lawrence Platform and Humber Zone and Silurian-Devonian Gaspé Belt successions, Quebec: Geological Survey of Canada, Open File 6050, 34 pages; 1 CD-ROM, doi:10.4095/288027

Lavoie, D., Hamblin, A. P., Thériault, R. Beaulieu J. and Kirkwood, D., 2008. The Upper Ordovician Utica Shales and Lorraine Group flysch in southern Québec: Tectonostratigraphic setting and significance for unconventional gas: Geological Survey of Canada, Open File 5900, 56 p.

Lavoie, D., J. Dietrich, N. Pinet, S. Castonguay, P. Hannigan, A.P. Hamblin and P.S. Giles, 2009. Hydrocarbon ressource assessment, Paleozoic basins of eastern Canada: Open File 6174, Geological Survey of Canada, 275 pages

Lavoie, D., Rivard, C. Lefebvre, R. Séjourné, S., Thériault, R., Duchesne, M. J., Ahad, J., Wang, B., Benoit, N. and Lamontagne, C. 2014. The Utica Shale and gas play in southern Quebec: Geological and hydrogeological syntheses and methodological approaches to groundwater risk evaluation: International Journal of Coal Geology, v. 126, p. 77-91, doi:10.1016/j.coal.2013.10.011

Lei, Y., Luo, X., Wang, X., Zhang, L., Jiang, C., Yang, W., Yu, Y., Cheng, M. and Zhang, L. 2015. Characteristics of silty laminae in Zhangjiatan Shale of southeastern Ordos Basin, China: Implications for shale gas formation; AAPG Bulletin, v. 99, no. 4 (April 2015), pp. 661–687.

Li, B, Mehmani, A,. Chen, J., Georgi, D. and Jin, G. 2013. The Condition of Capillary Condensation and Its Effects on Adsorption Isotherms of Unconventional Gas Condensate Reservoirs, SPE 166162, p.

Liu, D. Yuan, P., Liu, H., Li, T., Tan, D., Yian W., and He, H., 2013, High-pressure adsorption of methane on montmorillonite, kaolinite and illite, Applied Clay Science, v. 85, p.25–30. http://dx.doi.org/10.1016/j.clay.2013.09.009

Loucks, R.G., Reeds, R. M. Ruppel, S.C. and Jarvie, D. M. 2009. Morphology, genesis, and distribution of nanometer-scale pores in siliceous mudstones of the Mississippian Barnett shale: Journal of Sedimentary Research, v. 79, 848–861.

Loucks, R.G., Reeds, R. M., Ruppel, S. C. and Hammes, U. 2012. Spectrum of pore types and networks in mudrocks and a descriptive classification for matrix-related mudrock pores: AAPG Bulletin, v. 96, , p. 1071–1098

Loucks, R.G. and Reeds, R.M. 2014.Scanning-electron-microscope petrographic evidence for distinguishing organic-matter pores associated with depositional organic matter versus migrated organic matter in mudrocks: GCAGS Journal, v. 3, p. 51-60.

Lowe, D.G. and Arnott, R.W.C. 2016. Composition and architecture of braided and sheetflood-dominated ephemeral fluvial strata in the Cambrian-Ordovician Potsdam Group: A case example of the morphodynamics of early Phanerozoic fluvial systems and climate change: Journal of Sedimentary Research, v. 86, p. 587-612.

Lu, J., Ruppel, S. C. and Rowe, H. D. 2015. Organic matter pores and oil generation in the Tuscaloosa marine shale. AAPG Bulletin, v. 99, pp. 333–357.

Macauley, G. and Snowdon, L. R. 1984. A rock-Eval appraisal of the Ordovician Collingwood shales, southern Ontario: Geological Survey of Canada Open File 1092, 12p.

Marcil, J.S., Dorrins, P. K., Lavoie, J., Mechti, N. and Javoie, J.Y. 2012. Utica and Other Ordovician Shales: Exploration History in the Quebec Sedimentary Basins, Eastern Canada, Search and Discovery Article #10451.

Maugeri, L., 2015, Comment: Beware of break-even and marginal-cost analyses, Oil & Gas Journal, 02/10/2015, V. 3, Issue 1.

Michael, G.E., Packwood, J. and Holba, A. 2013. Determination of in-situ hydrocarbon volumes in liquid rich shale plays. Unconventional Resources Technology Conference, Denver, Colorado, USA, August 2013. http://www.searchanddiscovery.com/pdfz/documents/2014/80365michael/ndx_michael.pdf.html.

Milliken and Curtis, 2016. Imaging pores in sedimentary rocks: Foundation of porosity Prediction. Marine and Petroleum Geology, v.73, p.590-608. http://dx.doi.org/10.1016/j.marpetgeo.2016.03.020

Modica, C. J., and Lapierre, S. G. 2012. Estimation of kerogen porosity in source rocks as a function of thermal transformation: Example from the Mowry Shale in the Powder River Basin of Wyoming: AAPG Bulletin, v. 96, p. 87–108.

Noble R., Kaldi, J.G., and Atkinson, C.D. 1997. Oil saturations in Shales: Applications in Seal Evaluation. AAPG Memoir 67, p.13-29.

Obermajer, M., Fowler, M.G. and Snowdon, L. R., 1999. Depositional Environment and Oil Generation in Ordovician Source Rocks from Southwestern Ontario, Canada: Organic Geochemical and Petrological Approach, AAPG Bulletin, V. 83, P. 1426-1453.

Obermajer, M., Stewart, K. R. and Dewing, K. 2007.Geological and Geochemical Data from the Canadian Arctic Islands, Part II: Rock-Eval/TOC Data. Geological Survey of Canada, Open File 5459, 27 (+ fig.) p. (CD-ROM).

Pang, X., Li, M., Li, S., 2005. Geochemistry of petroleum systems in the Niuzhuang South Slope of Bohai Bay Basin: Part 3. Estimating hydrocarbon expulsion from the Shahejie formation. Organic Geochemistry, v.36, p.497–510.

Passey, Q.R., Creaney, S., Kulla, J. B., Moretti F. J. and Stroud, J. D. 1990. A practical model for organic richness from porosity and resistivity logs: AAPG Bulletin, v. 74, p. 1777-1794.

Passey, Q.R., Bohacs, K. M., Esch, W. L., Klimentidis, R. and Sinha, S. 2010. From oil-prone source rock to gas-producing shale reservoir – geological and petrophysical characterization of unconventional shale-gas reservoirs, SPE MS 131350, 29p.

Peters, K.E. 1986. Guidelines for evaluating petroleum source rock using programmed pyrolysis. American Association of Petroleum Geologists Bulletin, v. 70, no. 3, p. 318-329.

Peters, K.E., Walters C. C. and Moldowan, J. M. 2005. The biomarker guide, volume 1, Biomarkers and isotopes in the environment and human history, Cambridge University Press, Cambridge, UK. 471p.

Peters, K. E., Walters C. C. and Mankiewicz, P. J. 2006. Evaluation of kinetic uncertainty in numerical models of petroleum generation: AAPG Bulletin, v. 90, p. 387–403

Pommer, M. and Milliken, K. 2015. Pore types and pore-size distributions across thermal maturity, Eagle Ford Formation, southern Texas, AAPG Bulletin, v. 99, p. 1713–1744.

Ramm, M., 1991. Porosity – depth trends in reservoir sandstones: theoretical models related to Jurassic sandstone offshore Norway: Marine and petroleum geology, v. 9 p. 553-567.

Reed, R. M., Loucks, R. G., Ruppel, S. C., 2014. Comment on "Formation of nanoporous pyrobitumen residues during maturation of the Barnett Shale (Fort Worth Basin)" by Bernard et al. (2012). International Journal of Coal Geology v.127, p.111–113

Rexer, T. F. T., Benham, M. J. Aplin, A. C. and Thomas, K. M., 2013.Methane Adsorption on Shale under Simulated Geological Temperature and Pressure Conditions, Energy & Fuels, v. 27, p.3099−3109. dx.doi.org/10.1021/ef400381v

Romero-Sarmiento, M.F., Ducros, M., Carpentier, B., Lorant, F., Cacas, M. Ch., Pegaz-Fiornet, S., Wolf, S., Rohais, S. & Moretti, I. 2013. Quantitative evaluation of TOC, organic porosity and gas retention distribution in a gas shale play using petroleum system modeling: Application to the Mississippian Barnett Shale. Marine and Petroleum Geology 45: 315-330.

Romero-Sarmiento, M.F., Rouzaud, J.N., Bernard, S., Deldicque,D., Thomas, M. & Littke, R. 2014. Evolution of Barnett Shale organic carbon structure and nanostructure with increasing maturation. Organic Geochemistry v.71, p.7-16.

Romero-Sarmiento, M., Euzen, T., Rohais, S, Jiang, C. and Littke, R., 2016. Artificial thermal maturation of source rocks at different thermal maturity levels: Application to the Triassic Montney and Doig formations in the Western Canada Sedimentary Basin; Organic Geochemistry v.97, p.148–162.

Romero-Sarmiento, M.F, Pillot, D.,Letort,G.,Lamoureux-Var, V., Beaumont, V. Huc, V. and Garcia, B., 2015. New Rock-Eval Method for Characterization of Unconventional Shale Resource Systems, Oil & Gas Science and Technology – Rev. IFP Energies nouvelles, p.1-9.

Ross, D. J. K., and R. M. Bustin, 2009. The importance of shale composition and pore structure upon gas storage potential of shale gas reservoirs: Marine and Petroleum Geology, v. 26, p. 916–927.

Seewald, J. S. 2003. Organic–inorganic interactions in petroleum-producing sedimentary basins, Nature V. 426 | 20 Nov. 2003 | www.nature.com/nature. http://www.nature.com/nature/journal/v426/n6964/pdf/nature02132.pdf

Séjourné, S., R. Lefebvre, X. Malet and D. Lavoie, 2013. Geological and hydrogeological synthesis of the Utica Shale and units overlying (Lorraine, Queenston and surficial), lowland of Saint-Laurent, Province of Quebec: Geological Survey of Canada, Open File 7338, 165p.

Slatt R. M. and OBrien, N. R. 2011. Pore types in the Barnett and Woodford gas shales: Contribution to understanding gas storage and migration pathways in fine-grained rocks: AAPG Bulletin, v. 95, p. 2017–2030.

Snowdon, L, 1995. Rock-Eval T_{max} suppression; documentation and amelioration: AAPG Bulletin, v. 79, p. 1337-1348.

Thériault, R., 2012a. Caractérisation du Shale d'Utica et du Groupe de Lorraine, Basses-Terres du Saint-Laurent - Partie 1 : Compilation des données : Ministère des Ressources naturelles et de la Faune, Québec; DV 2012-03, 212 p.

Thériault, R., 2012b. Caractérisation du Shale d'Utica et du Groupe de Lorraine, Basses-Terres du Saint-Laurent - Partie 2 : Interprétation géologique : Ministère des Ressources naturelles et de la Faune, Québec; DV 2012-04, 80 ps.

Tian, H., Xiao, X., Wilkins, R. W. T. and Tang, Y., 2008. New insights into the volume and pressure changes during the thermal cracking of oil to gas in reservoirs: Implications for the in-situ accumulation of gas cracked from oils: AAPG Bulletin, v. 92, p. 181–200.

Tissot; B.P. and Welte, D. H. 1984, Petroleum Formation and Occurrence: Springer-Verlag, New York, 699pp.

Wang, F. P., Hammes, U., Reeds, R. Zhang, T. ,Tang X. and Li, Q. 2013. Petrophysical and mechanical properties of organic-rich shales and their influences on fluid flow, *in* J. Chatellier and D. Jarvie, eds., Critical assessment of shale resource plays: AAPG Memoir 103, p. 167–186.

Wang, S., Feng, Q., Zha, M, Lu, S., Qing, Y., Xiao., T. and Zhang, C., 2015. Molecular dynamics simulation of liquid alkane occurrence state in pores and slits of shale organic matter. Petroleum Exploration and Development, v. 42, p.844-851.

Wang, J., Luo, H., Liu, H., Lin, J., Li. And Lin, W., 2016. Influences of adsorption/desorption of shale gas on the apparent properties of matrix pores. Petroleum Exploration and Development, 43(1): p.158–165. http://www.sciencedirect.com/science/journal/18763804/43/1.

Wang, P., Chen. Z., Pang, X., Hu, K., Sun, M. and Chen, X. 2016. Revised models for determining TOC in shale play: Example from Devonian Duvernay Shale, Western Canada Sedimentary Basin, Marine and Petroleum Geology, v. 70, p.304-319.

Wang, P, Chen, Z., Pang, X., Jiang, C., Sun, M. and Chen, X., 2016, Petroleum System Modeling of Devonian Duvernay Formation, Western Canada Sedimentary Basin: Implication for Shale Oil and Gas Resources, AAPG Annual Convention & Exhibition, June 19-22, 2016, Calgary, Alberta, Canada.

Wang, S., Song, Z., Cao, T., and Song, X., 2013. The methane sorption capacity of Paleozoic shales from the Sichuan Basin, China, Marine and Petroleum Geology v.44, p.112-119

Williams, K. E., 2013. Source Rock Reservoirs are a Unique Petroleum System, Search and Discovery Article #41138 (2013).
http://www.searchanddiscovery.com/pdfz/documents/2013/41138williams/ndx_williams.pdf.html

Wood, J. M., Sanei, H. Curtis M.E. and Clarkson, C. R. 2015. Solid bitumen as a determinant of reservoir quality in an unconventional tight gas siltstone play, International Journal of Coal Geology, v.150-151, p.287-295.

Yu, W., Sepehmoori, K., and Patzek, T.W., 2015. Modeling gas adsorption in Marcellus Shale with Langmuir and BET isotherms, SPE 170801, SPE Journal, p.1-12.

Zhang, T, Ellis, G. S., Ruppel, S. C., Milliken K. and Yan, R. 2012. Effect of organic-matter type and thermal maturity on methane adsorption in shale-gas systems: Organic Geochemistry v. 47, p. 120–131.

Zhao, H., Givens N. B. and Courtis, B. 2007. Thermal maturity of Barnett shale determined from well-logs analysis: AAPG Bulletin, v. 91, p. 535-549.

Figure Captions

Figure 1. Schematic diagram showing the two different porosity trends in a shale play (matrix porosity and organic porosity). The two pore systems result from different geological processes and show different evolution histories. The matrix porosity curve is based on a generalized compaction model from sonic logs from the Duvernay Formation in Western Canada Sedimentary Basin, and a constant initial total organic carbon (iTOC) of 8% is based on initial TOC estimation of the same formation (Chen and Jiang, 2016)..

Figure 2. a) Matrix porosity dominated system (e.g. Montney) shows a negative correlation between TOC and porosity; whereas organic porosity dominant system (e.g. Doig) shows a positive correlation (Jarvie, 2012b); b) A plot of water saturation against TOC in organic rich shale (U.S shale data from Wang et al, 2013).

Figure 3. A petrophysical model of a tight-shale play where both matrix and organic porosities contribute to the storage of oil and gas (modified from Ambrose et al. 2012). The percentage of the various components forming the bulk of the rock volume is schematic and does not intent to represent a specific case.

Figure 4. A work-flow chart showing the components and procedures in hydrocarbon pore volume evaluation using geochemical and well log data under the dual-porosity model. SR: Source Rock; HC: Hydrocarbon; TOC: Total Organic Carbon (w%).

Figure 5. A regional geological map of southern Quebec with the Cambrian-Ordovician St. Lawrence Platform between the Precambrian Grenville basement to the northwest and the Cambrian-Devonian

Appalachians to the southeast. Logan's line marks the limit between the platform and the Appalachians whereas the platform is either in fault contact or unconformably overlying the Grenvillian basement. The locations of oil and gas well drilled in southern Quebec are shown as red circles and recent shale gas wells shown as black circles. Figure modified from Thériault (2012a).

Figure 6. Stratigraphic framework of the St. Lawrence Platform of southern Quebec with interpreted tectono-stratigraphic episodes.

Figure 7. Map showing locations of data wells and oil and gas shows in Utica Shale gas in southern Quebec. Thermal maturity level of the Utica shale is indicated by color in five different hydrocarbon zones (modified from Séjourné et al. 2013).

Figure 8. Maps showing major geological features of the Utica Shale in the study area. a) Utica Shale thickness in meter; b) Burial depth in meter to the top of Utica Shale; c) Average present-day TOC content in weight % and d) Vitrinite reflectance equivalent in %. White crosses indicate location of data well. Data available at the Département of Ressources Naturelles du Quebec Oil and Gas SIGPEG database; http://sigpeg.mrn.gouv.qc.ca/gpg/classes/igpg

Figure 9. a) T_{max} vs HI plot showing hydrocarbon generation potential as a function of thermal maturity and kerogen thermal decomposition behaviour; data include the mature Utica Shale and the less mature, time- and facies-equivalent Collingwood Member of southern Ontario; b) Comparison of the estimated transformation ratio (TR) from T_{max} with the transformation ratio model of Bordenave et al. (1993) and data; c) Plot of Bitumen Index Equivalent (defined as BIE=S1/TOC*100) against T_{max}. The hydrogen generation index (HGI) showing onset of oil generation, peak generation and thermal cracking of oil to natural gas; d) Comparison of TR and expulsion efficiency models constructed using the Rock-Eval dataset.

Figure 10. Kriged resource maps of the Utica Shale in the study area showing the spatial variation of the estimated hydrocarbon resources across southern Quebec, Canada. a) Hydrocarbon pore volume (color bar: thickness (in meters) of hydrocarbons/unit area); b) In-place oil resource density (color bar: 10^6 bls/section); c) Resource density map for the adsorbed gas (color bar: bcf/section); d) Resource density map for the total natural gas (color bar: in bcf/section). Cross: data well location.

Figure 11. Statistical distributions of the estimated in-place oil resource showing the uncertainty of the estimate based on 6000 Monte Carlo runs. a) Histogram and b) Cumulative probability distribution.

Figure 12. Statistical distributions of the estimated in-place gas resource showing the uncertainty in the resource estimates based on 6000 Monte Carlo runs: histogram (left) and cumulative probability distribution (right). a) and b) Free gas; c) and d) Solution gas; e) and f) Adsorbed gas and g) and h) Aggregated total natural gas.

Figure 13. Probability distribution of the estimated natural gas in-place resources showing the relative contributions from the three different types of gas (free, solution and adsorbed) in the Utica Shale. Free gas dominates the distribution.

Table Captions

Table 1 Summary table of oil and gas resource estimates as cumulative distribution in the Utica Shale in southern Quebec, Canada. Probability distributions indicate large uncertainties for the resource potential due to insufficient data and our understanding of the shale play.

Table 2 Distributions of in-place resource potential of different gas components and the aggregated total in-place gas potential in Utica Shale, Quebec.

Table 1

Probability Distribution	95%	90%	75%	50%	25%	10%	5%	Mean
Oil in-place (Billion Barrels)	0.69	0.83	1.11	1.55	2.22	3.06	3.72	1.80
Aggregated gas in-place (TCF)	101.50	110.53	129.42	155.61	188.07	228.13	258.32	163.99

Table 2

Probability Distribution	95%	90%	75%	50%	25%	10%	5%	Mean
Adsorbed gas (TCF)	24.69	27.52	32.47	39.00	46.99	55.59	61.23	40.52
Free gas (TCF)	47.44	53.66	65.61	83.67	109.50	140.51	163.34	91.91
Solution gas (TCF)	19.98	21.36	24.18	28.68	35.56	44.35	51.05	31.25

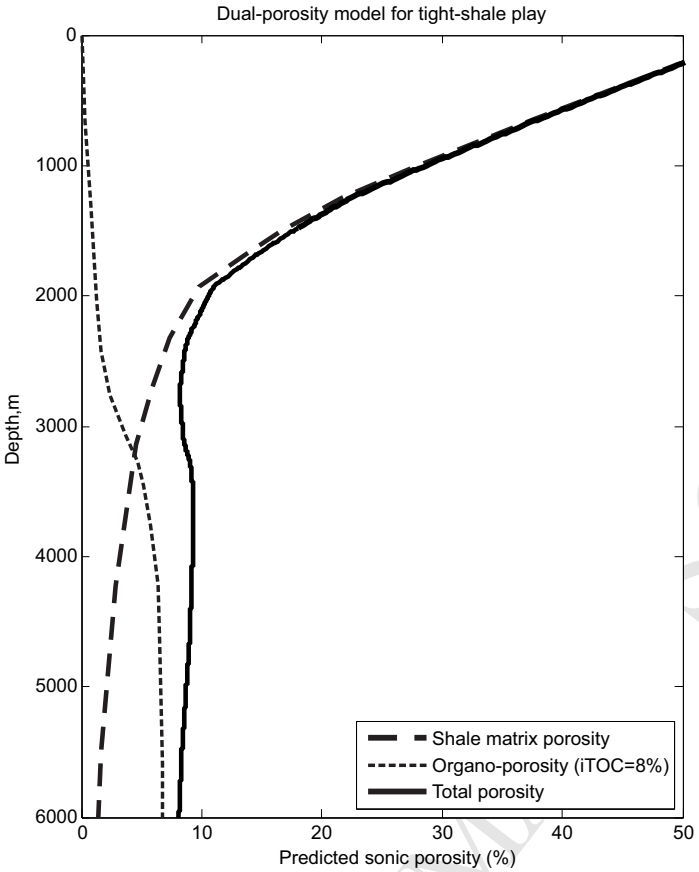

Figure 1

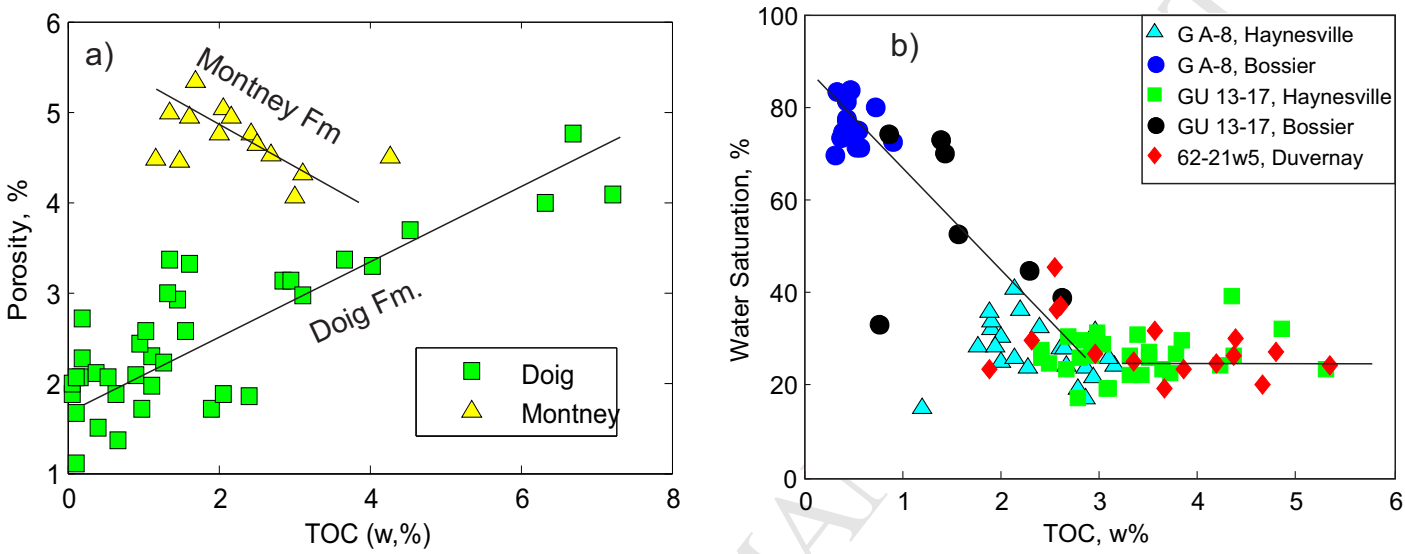

Figure 2

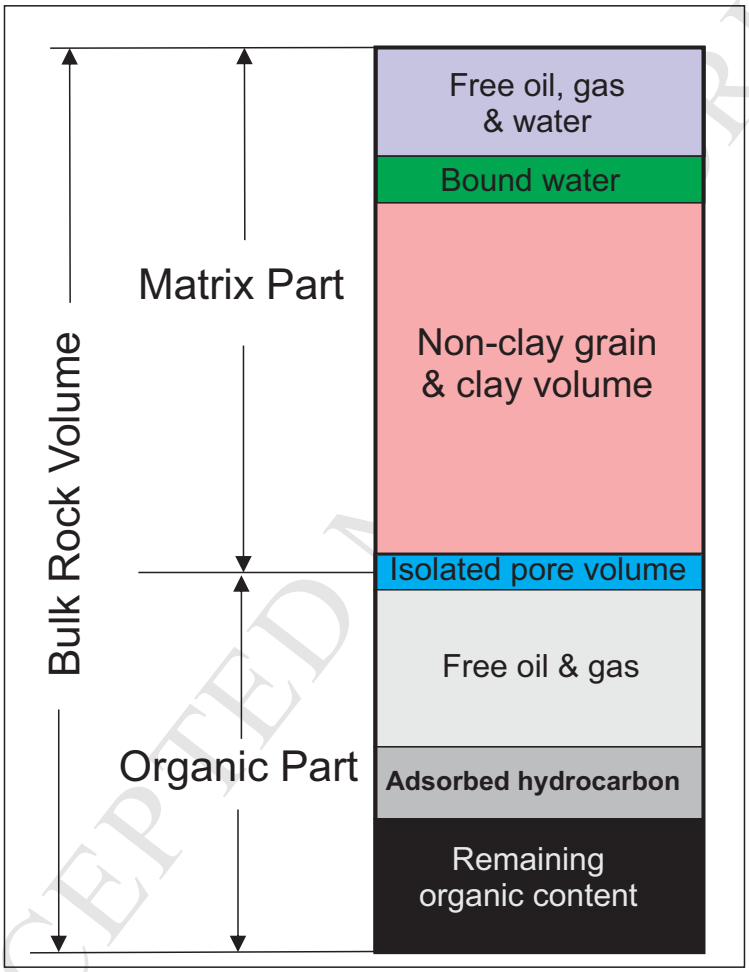

Figure 3

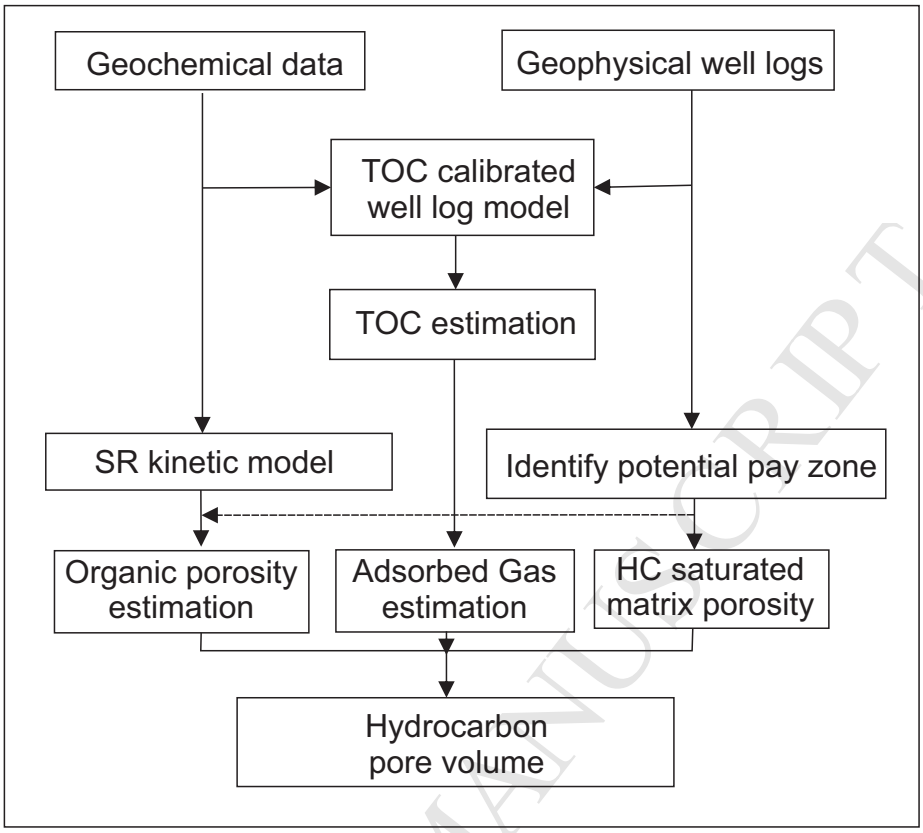

Figure 4

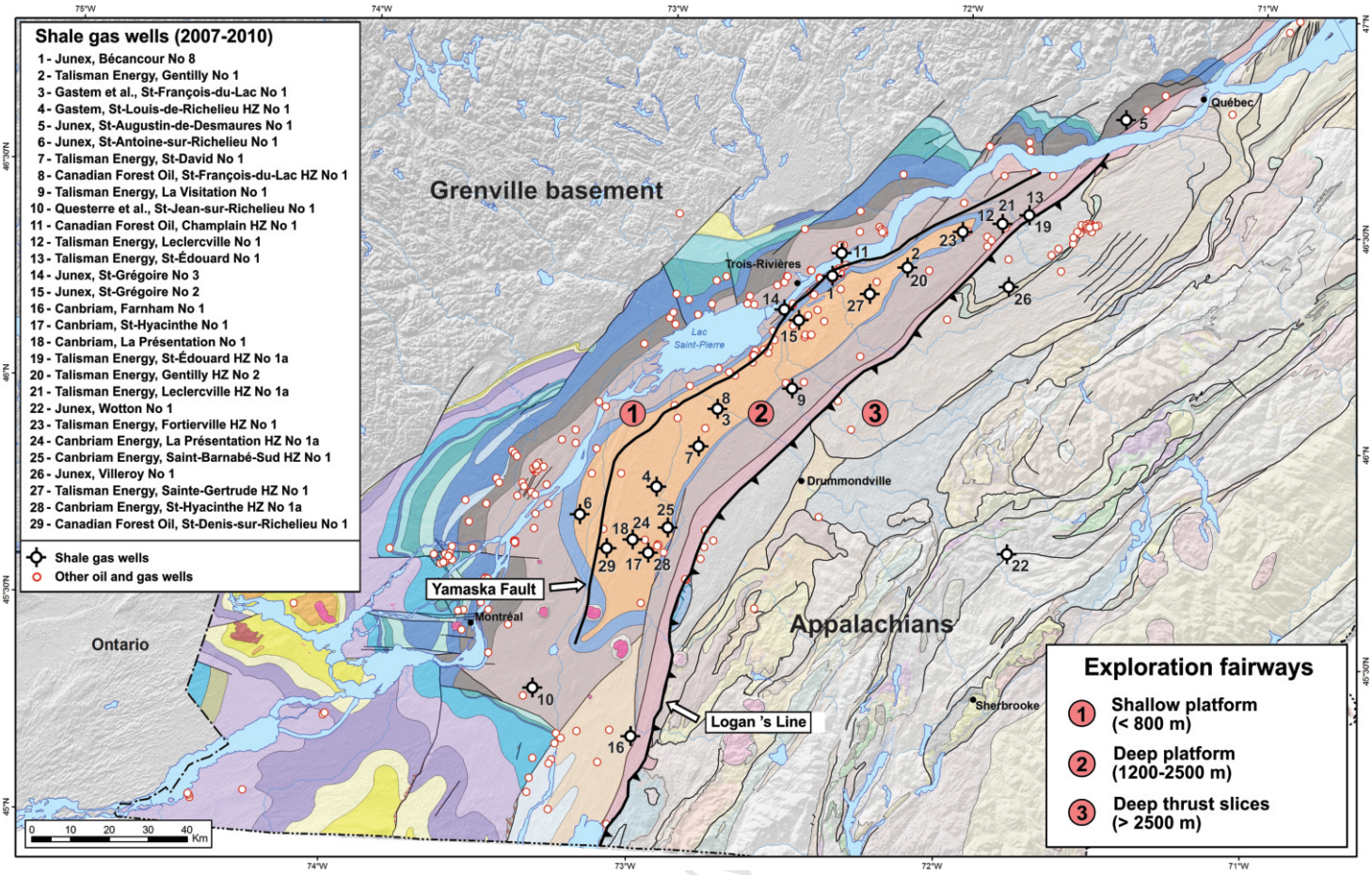

Figure 5

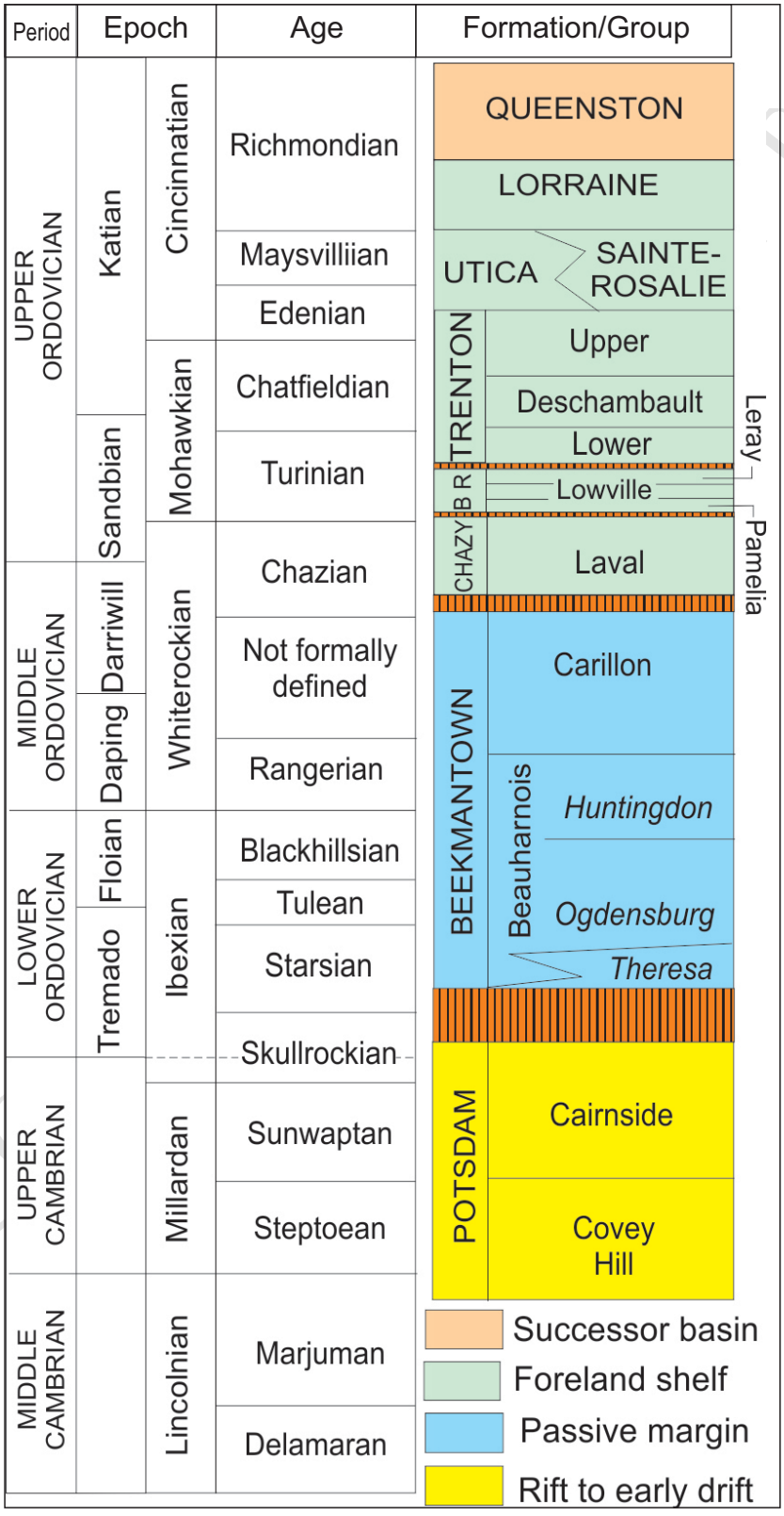
Period
Epoch
Age
Formation/Group
UPPER ORDOVICIAN
MIDDLE ORDOVICIAN
LOWER ORDOVICIAN
UPPER CAMBRIAN
MIDDLE CAMBRIAN
Katian
Sandbian
Darriwill
Daping
Floian
Tremado
Cincinnatian
Mohawkian
Whiterockian
Ibexian
Millardan
Lincolnian
Richmondian
Maysvilliian
Edenian
Chatfieldian
Turinian
Chazian
Not formally defined
Rangerian
Blackhillsian
Tulean
Starsian
Skullrockian
Sunwaptan
Steptoean
Marjuman
Delamaran
QUEENSTON
LORRAINE
UTICA
SAINTE-ROSALIE
TRENTON
Upper
Deschambault
Lower
B R
Lowville
CHAZY
Laval
BEEKMANTOWN
Carillon
Beauharnois
Huntingdon
Ogdensburg
Theresa
POTSDAM
Cairnside
Covey Hill
Leray
Pamelia
Successor basin
Foreland shelf
Passive margin
Rift to early drift

Figure 6

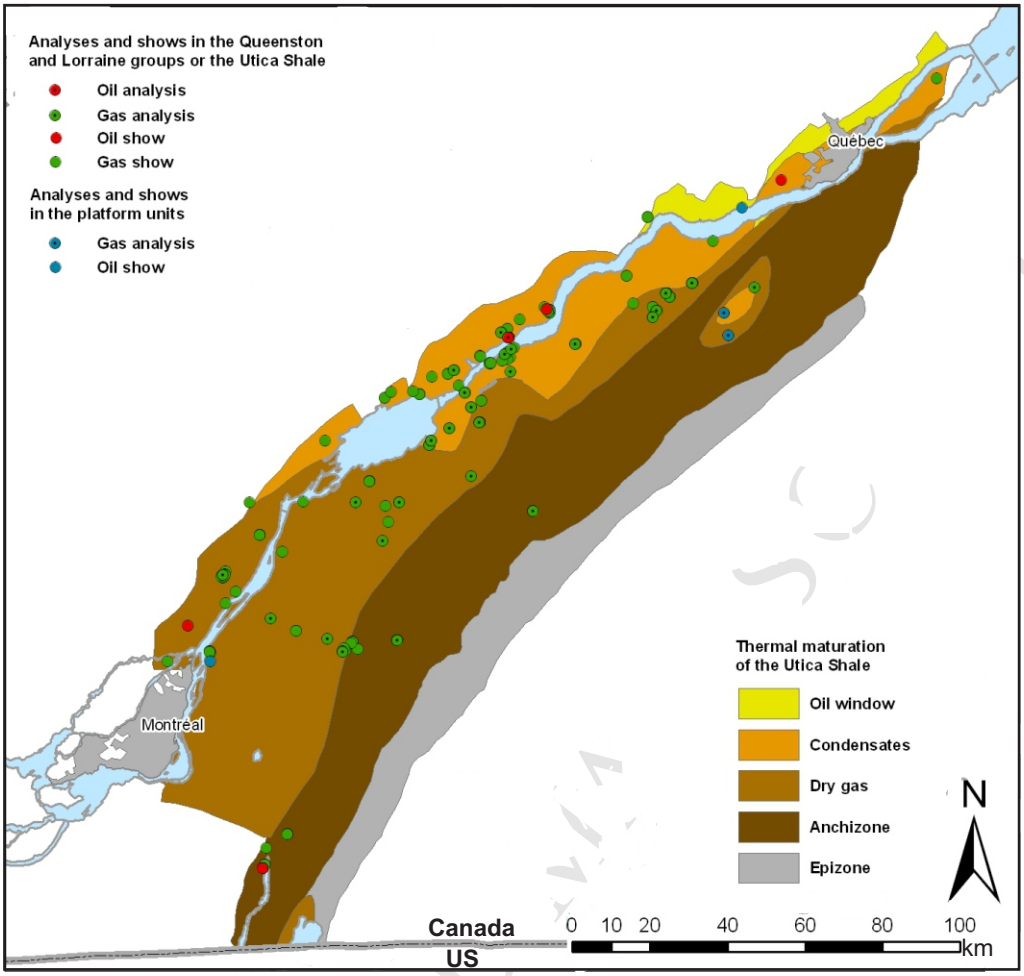
Analyses and shows in the Queenston and Lorraine groups or the Utica Shale
Oil analysis
Gas analysis
Oil show
Gas show
Analyses and shows in the platform units
Gas analysis
Oil show
Québec
Montréal
Thermal maturation of the Utica Shale
Oil window
Condensates
Dry gas
Anchizone
Epizone
N
Canada
US
0 10 20 40 60 80 100
km

Figure 7

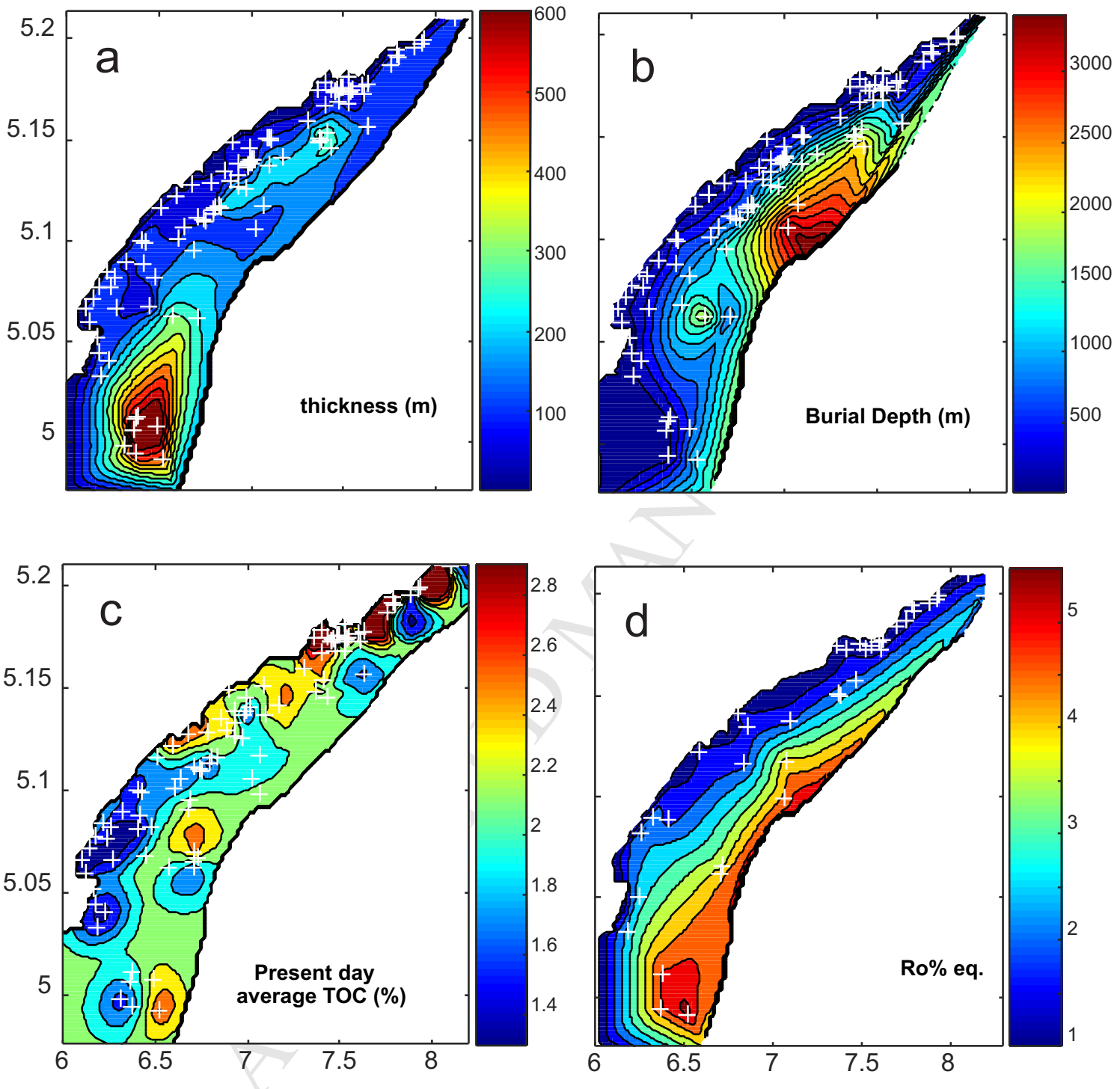
a
thickness (m)
600
500
400
300
200
100
b
Burial Depth (m)
3000
2500
2000
1500
1000
500
c
Present day
average TOC (%)
2.8
2.6
2.4
2.2
2
1.8
1.6
1.4
d
Ro% eq.
5
4
3
2
1
5.2
5.15
5.1
5.05
5
6
6.5
7
7.5
8

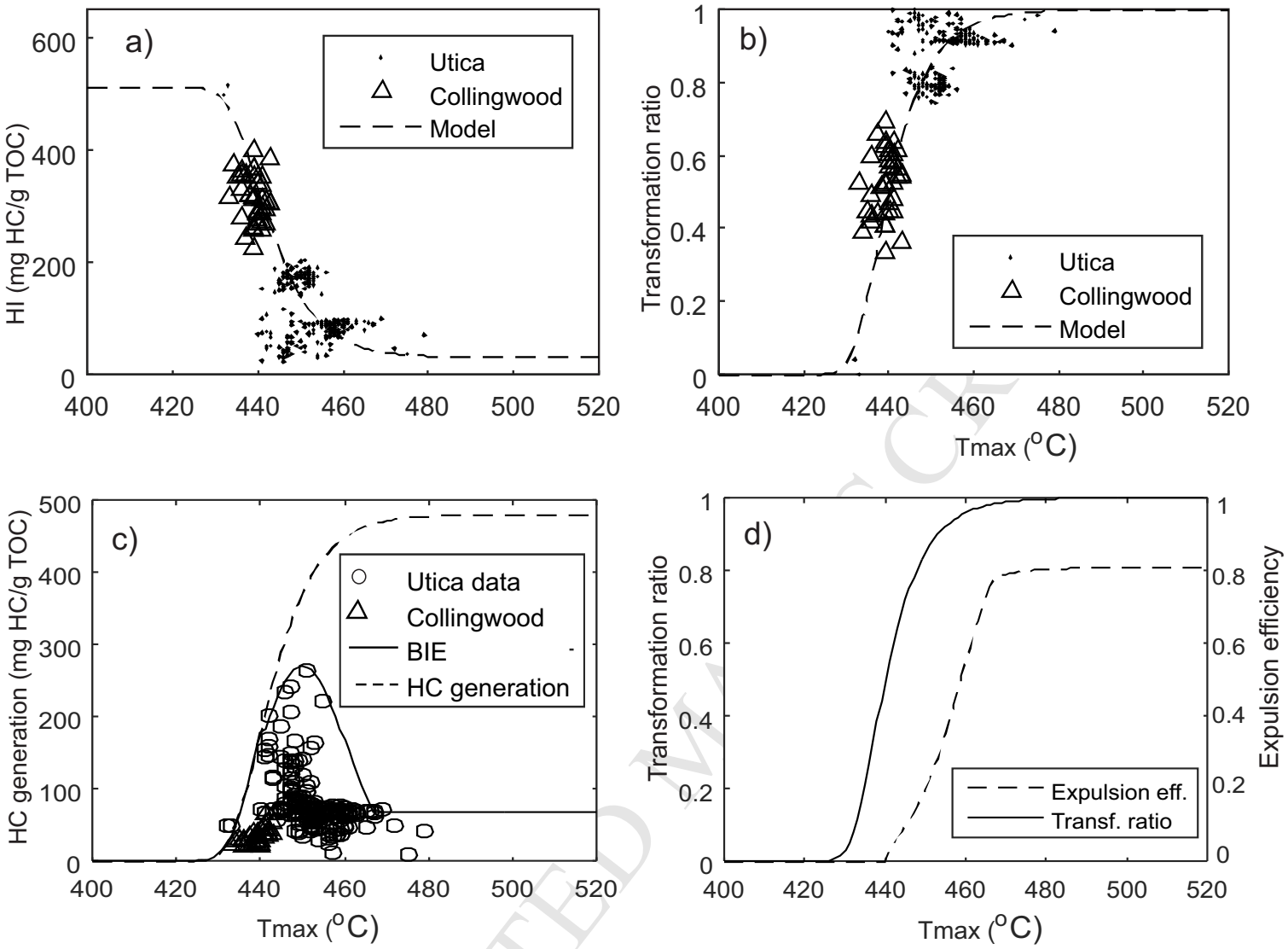

Figure 9

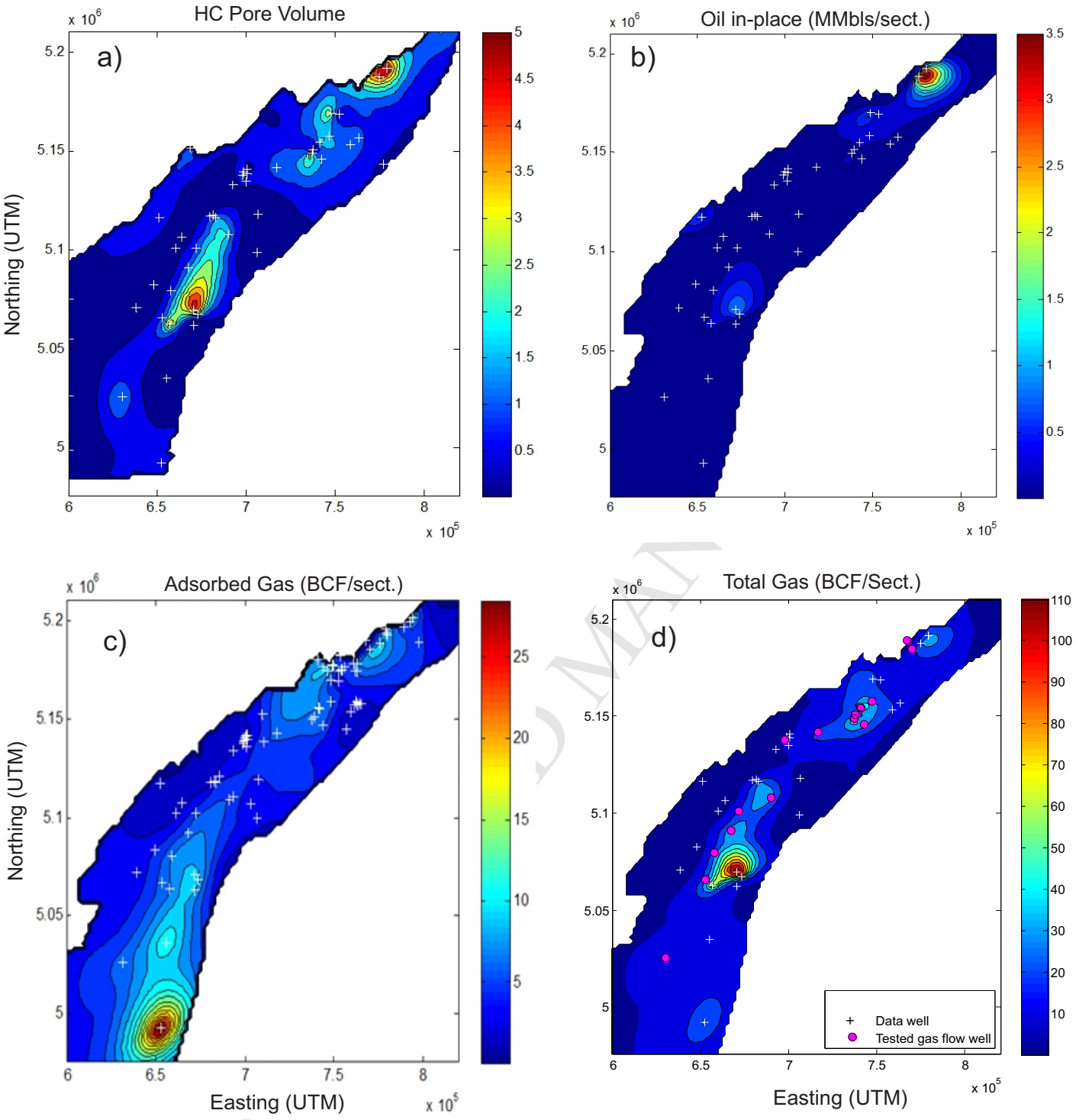
HC Pore Volume
a)
Oil in-place (MMbls/sect.)
b)
Adsorbed Gas (BCF/sect.)
c)
Total Gas (BCF/Sect.)
d)
Northing (UTM)
Easting (UTM)
x 10^6
x 10^5
Data well
Tested gas flow well

Figure 10

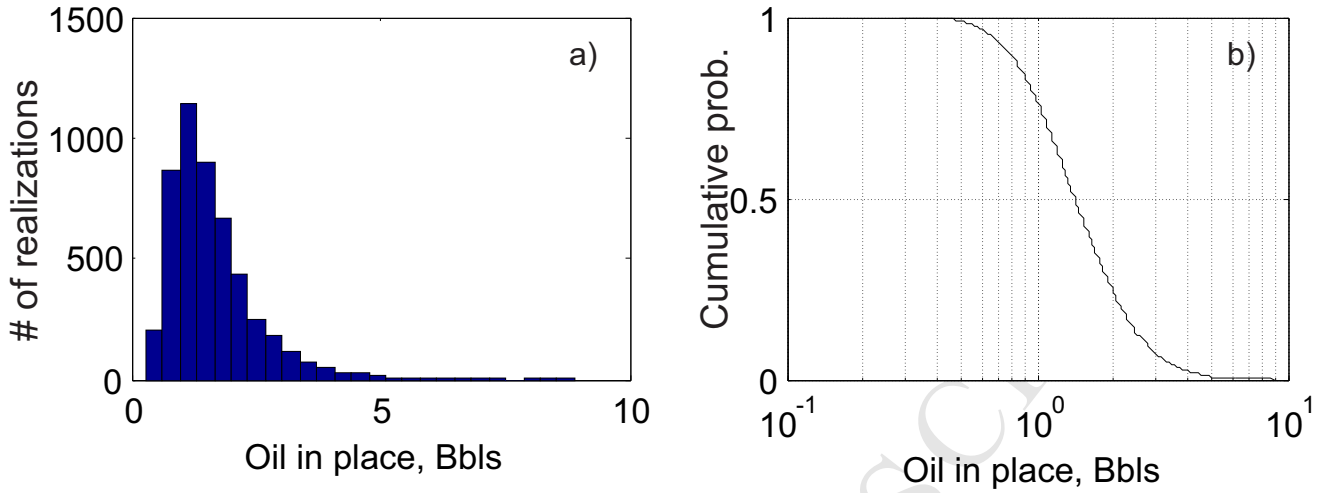

Figure 11

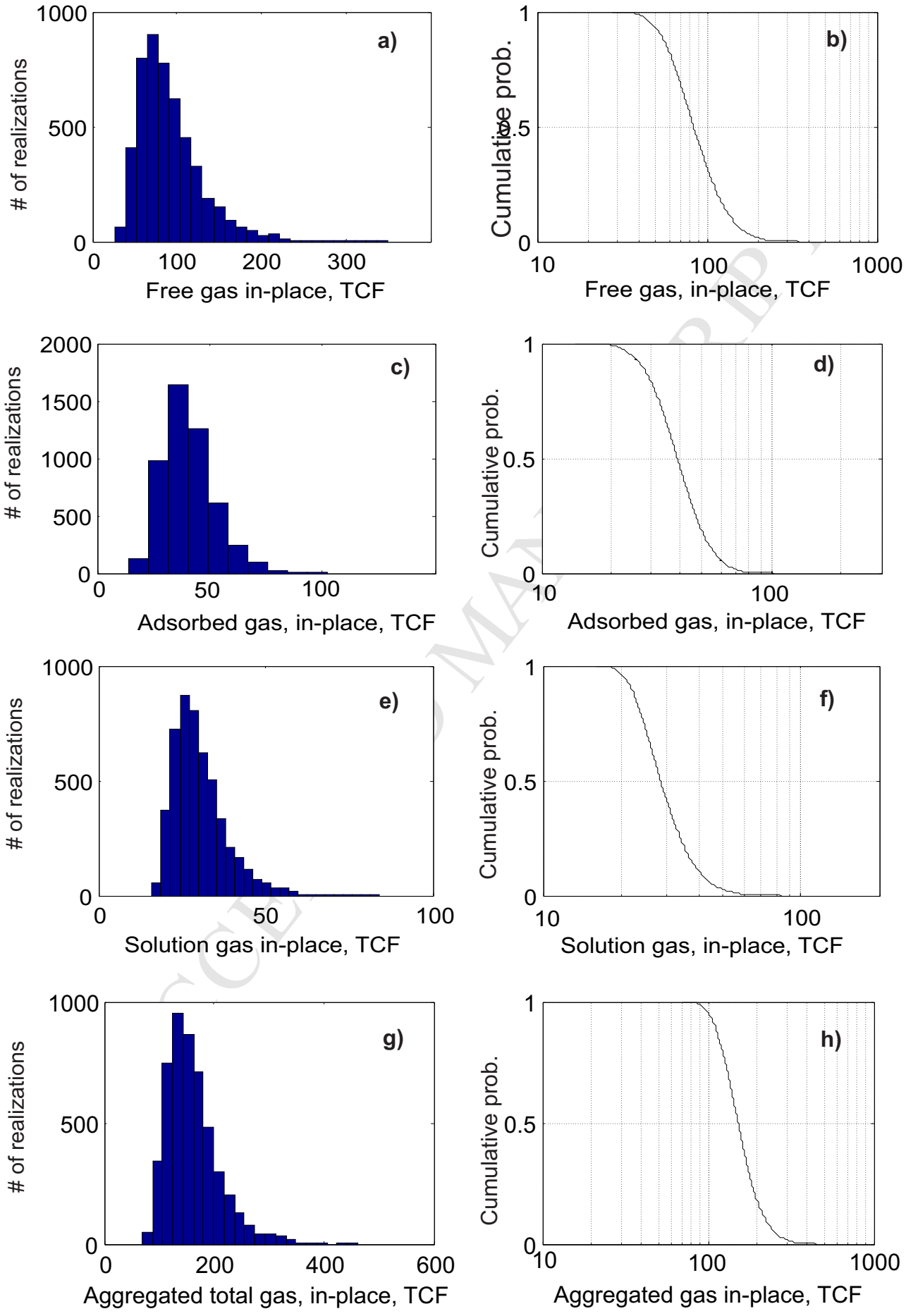
a)
# of realizations
Free gas in-place, TCF
b)
Cumulative prob.
Free gas, in-place, TCF
c)
# of realizations
Adsorbed gas, in-place, TCF
d)
Cumulative prob.
Adsorbed gas, in-place, TCF
e)
# of realizations
Solution gas in-place, TCF
f)
Cumulative prob.
Solution gas, in-place, TCF
g)
# of realizations
Aggregated total gas, in-place, TCF
h)
Cumulative prob.
Aggregated gas in-place, TCF

Figure 12

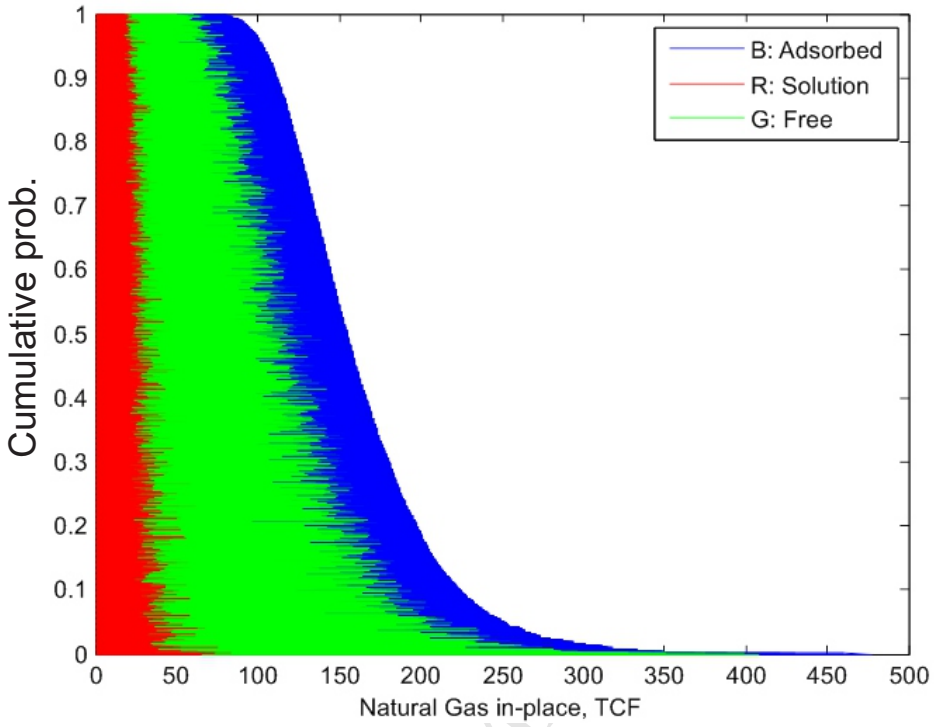

Figure 13